ACR No. 5K27

NATIONAL ADVISORY COMMITTEE FOR AERONAUTICS

WARTIME REPORT

ORIGINALLY ISSUED

March 1946 as
Advance Confidential Report 5K27

THEORY AND APPLICATION OF HOT-WIRE INSTRUMENTS IN THE INVESTIGATION OF TURBULENT BOUNDARY LAYERS

By G. B. Schubauer and P. S. Klebanoff
National Bureau of Standards

NACA

WASHINGTON

NACA ACR No. 5K27

NATIONAL ADVISORY COMMITTEE FOR AERONAUTICS

ADVANCE CONFIDENTIAL REPORT

THEORY AND APPLICATION OF HOT-WIRE INSTRUMENTS IN THE INVESTIGATION OF TURBULENT BOUNDARY LAYERS

By G. B. Schubauer and P. S. Klebanoff

SUMMARY

An account is given of the recent developments in hot-wire instruments for use in turbulent boundary layers to determine the magnitude of the several components of the turbulent velocity fluctuations together with the correlation between them and turbulent shearing stress. The instruments were developed in order to make possible a study of the turbulent characteristics of the layer as well as the average characteristics in a general investigation of the turbulent boundary layer under conditions producing separation. The experimental setup used to provide a thick turbulent boundary layer is described, and results are included to show the general nature of the boundary layer, as well as examples of the measured fluctuations, correlation coefficient, and turbulent shearing stress. Finally the errors inherent in the hot-wire method are discussed.

I. INTRODUCTION

The object of this investigation of the characteristics of turbulent boundary layers is to provide a sound basis of understanding of the turbulent type of boundary layer through careful study of its development and separation. The investigation involves the measurement of pressure distribution, distribution of mean velocity across the layer, boundary layer thickness, and shape parameter, as well as measurements of the turbulent characteristics of the layer.

While a considerable fund of information exists on the mean flow in turbulent boundary layers, little is known about the turbulence itself. All concerned with the boundary-layer problem agree, however, that turbulent mixing processes are

the fundamental processes in the boundary layer and contain the explanation of such average characteristics as velocity distribution, internal friction or shearing stress, and separation in an adverse pressure gradient. It is therefore not for lack of importance that turbulence measurements have been neglected, but rather from a lack of suitable instruments and techniques for making the necessary measurements. When the present boundary-layer investigation was undertaken, it was decided to determine as many characteristics of the turbulence as possible, along with the average characteristics of the layer, to fill in the gap left by former investigators. In order to make the turbulence measurements, it has been necessary first to develop some special type of hot-wire anemometer instruments. The present report covers research on development of the various hot-wire instruments and their adaptation to the turbulent boundary-layer investigation.

In order to see what turbulent characteristics of the layer should be measured to best further an understanding of turbulent boundary layers, it is well to look into the usual boundary-layer concepts associated with turbulence. It is customary to think in terms of the velocity fluctuations and to regard these fluctuations as the velocity of migration of fluid masses relative to the mean flow. The three mutually perpendicular components of the fluctuations are denoted here by u, v, and w and are defined under Symbols in the following section. As expressed by Von Kármán in reference 1, the main characteristics of turbulent flow at a given point are the magnitudes of the fluctuations and the correlation between them. The average product of the fluctuations, as, for example, uv, multiplied by the density are the turbulent shearing stresses. Momentum transfer, which gives rise to the shearing stresses, involves the concept of a length, or characteristic size, of the region involved in the turbulent exchange. The descriptive term "mixing length" to denote this characteristic length was first used by Prandtl.

The migratory processes are imagined to be somewhat analogous to those involved in the kinetic theory of gases, with the turbulent motions corresponding in the analogy to molecular motions in a gas and the mixing length corresponding to the mean free path. While such concepts have been in use for many years, little is known about the actual nature of the processes, and assumptions about them have had to be made in formulating fundamental laws. In relatively simple cases, such as turbulent flow in pipes and turbulent boundary layers on plane surfaces, the assumptions have yielded formu-

las for mean velocity distribution in fair agreement with experiment; but in cases where a turbulent boundary layer develops under the combined action of friction and large pressure gradients, the usual assumptions lead to erroneous results and are obviously not valid. This is particularly true in large adverse pressure gradients, and it is here that the greatest need arises for an understanding of the actual nature of the turbulent processes.

There is need, therefore, for experimental determinations of the magnitude of the various components of the fluctuations, the correlation between components, the turbulent shearing stresses, and mixing lengths in turbulent boundary layers. These will provide the basic information on which to base laws governing the mean motion and the development of the layer. The object in instrument development has been to obtain the means for making measurements that will permit the determination of as many of these quantities as possible.

This investigation, conducted at the National Bureau of Standards, was sponsored by and conducted with the financial assistance of the National Advisory Committee for Aeronautics.

II. SYMBOLS

U_o free-stream velocity, defined here as the velocity that would exist in the region occupied by the wall with the wall absent

q_o free-stream dynamic pressure corresponding to U_o

U local mean velocity at any point

U_1 particular local mean velocity just outside of boundary layer

x distance along surface measured from the forward stagnation point

y distance normal to surface, measured from the surface

z coordinate normal to x and y with origin on the center line (In the two-dimensional case considered here, mean flow conditions do not vary in the z-direction.)

x,y,z	coordinates of a point in boundary layer
xy–plane	plane of mean flow
xz–plane	plane normal to xy–plane and tangent to local direction of mean flow at all points
u	x–component of velocity fluctuation lying in xy– and xz–plane
v	y–component of velocity fluctuation lying in xy–plane
w	z–component of velocity fluctuation lying in xz–plane
u', v', w'	root–mean–square values of u, v, and w; that is, $u' = \sqrt{\overline{u^2}}$, $v' = \sqrt{\overline{v^2}}$, $w' = \sqrt{\overline{w^2}}$, where the bar denotes mean value. The primed symbols are used to avoid an awkward notation in equations
$\overline{uv}$	mean value of product of u and v
φ	angle between axis of hot wire and direction of wind at the location of the wire
h	rate of heat loss from hot wire, watts per second
T	instantaneous temperature of wire
T_e	equilibrium temperature of wire
$\overline{T}$	mean temperature of hot wire, degrees C
T_a	air temperature, degrees C; also temperature of wire when unheated
R	mean resistance of hot wire at temperature $\overline{T}$, ohms
R_a	resistance of wire at temperature T_a, ohms
R_o	resistance of unheated wire at 0° C
τ_o	resistivity of the material of the wire at 0° C

α	temperature coefficient of resistance referred to 0° C
$R_0\alpha$	slope of temperature-resistance curve
i	current through hot wire
$E = iR$	mean voltage across hot wire (When two wires are used, E_1 denotes mean voltage across wire I and E_2 denotes mean voltage across wire II.)
$E_a = E_1 + E_2$	sum of mean voltage across pair of wires
$E_b = E_1 - E_2$	difference of mean voltage across pair of wires
ΔE_b	change in E_b per radian
e	(with various subscripts) voltage fluctuation compensated for wire lag
t	time
M_0	lag constant of wire
M	time constant, seconds
γ	phase angle
f	frequency, cycles per second
m	mass of the hot wire
s	specific heat of material of the wire
ρ_1	density of material of the wire
r	radius of wire
ρ	density of air, slugs per cubic foot
μ	viscosity of air, slug ft^{-1} sec^{-1}
$\nu = \mu/\rho$	kinematic viscosity of air, ft^2 sec^{-1}
$\tau = -\rho\,\overline{uv}$	shearing stress, pound per square foot

τ_o shearing stress on the surface or skin friction

$c_f = \tau/1/2\ \rho U_1^2 = 2\overline{uv}/U_1^2$ friction coefficient

$K = \overline{uv}/u'v'$ correlation coefficient

l mixing length

δ boundary-layer thickness

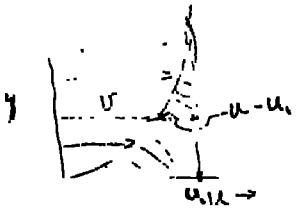

δ^* displacement thickness $\left(\int_0^\infty \left(1 - \frac{U}{U_1}\right) dy\right)$ $\frac{a_1 - v}{v_1}$

θ momentum thickness $\left(\int_0^\infty \frac{U}{U_1}\left(1 - \frac{U}{U_1}\right) dy\right)$

$H = \delta^*/\theta$ shape parameter

C chord of wall, 27.9 feet

x_s position of separation point

$RN = U_o C/\nu$ Reynolds number

III. THE NATURE OF THE PROBLEMS INVOLVED

The so-called "turbulence wire," consisting of a hot-wire anemometer with a single wire normal to the wind, has been successfully used in the past in both laminar and turbulent boundary layers to measure the u-component of the fluctuations. An attempt was made about 1937 by H. K. Skramstad to determine v- and w-components of the fluctuations in a turbulent layer by the method of thermal diffusion. (Results unpublished. Method and theory given in references 2 and 3.) He found that the interpretation of results was uncertain because of effects of velocity gradient. Skramstad found, however, that a hot-wire anemometer with the wire making an angle of about 45° to the wind could be used with apparent success to measure turbulent shearing stress (reference 4). In recent years, specially constructed

hot-wire anemometers have taken the place of thermal diffusion apparatus and have found considerable use in the measurement of the cross-stream component of turbulence in wind tunnels. Early attempts to use these instruments in turbulent boundary layers, while not entirely successful, indicated at least that under proper conditions reliable results should be obtainable. The principal condition was that the instruments be small compared to the thickness of the boundary layer. This same condition applies to the measurement of shearing stress.

On the basis of this experience an investigation of the turbulent boundary layer again was undertaken. The requirements of the experimental setup were that the boundary layer should be as thick as possible in order to avoid the necessity of building hot-wire instruments vanishingly small and that the adverse pressure gradient parallel to the surface should be sufficiently large to produce separation and yet be negligible normal to the surface. This required a long surface with small curvature, and accordingly the "wall" shown in figure 1 was constructed in the National Bureau of Standards' largest wind tunnel, namely the 10-foot open-air tunnel. The shape and dimensions of this wall are shown in figure 2. The working side, which is the side with curvature on the downstream end, has a smooth surface 28 feet long. The blister on the side of the tunnel was added to steepen the pressure rise and produce separation at the point indicated. By suitable control of the secondary flow near the floor, the flow along the central section was rendered two-dimensional up to and somewhat beyond the separation point.

During the course of the investigation difficulties were encountered with the hot-wire instruments. While the primary cause of the difficulties was the dirt and flying particles carried by the wind, the difficulties manifested themselves in such a way as to show that the requirements for accurate measurements had not been fully appreciated at the outset of the investigation. For example, flying particles broke and bent the delicate platinum wires used as the sensitive element on all hot-wire instruments. Screening the entrance to the tunnel improved matters somewhat, but collisions with smaller particles still getting through the screen bent the wires and changed the calibration of those instruments the characteristics of which depended on the angle between the wire and the wind. Platinum wires could not be placed under tension, and an impact, however slight, with a solid body changed the shape of the wire. In fact, it has since become

clear that it was only a matter of good fortune that measurements of shearing stress were ever possible without having the wire under tension to insure constancy of angle. Another difficulty equally detrimental to accuracy was the accumulation of dirt on the wires.

While these difficulties were probably at their worst in an open-air wind tunnel, they were of such a nature as to indicate that the hot-wire instruments generally might not be practicable for all the measurements theoretically possible. Having found the requirements to be met by a suitable instrument, new methods of construction were tried using tungsten wire and the performance of these new types was investigated in detail. As the result, satisfactory instruments were found, and methods of reducing observed data were improved on the basis of more complete information on the characteristics of such instruments. Thus the stage has been reached where it is possible to state what measurements are possible in practice as well as in theory and give an estimate of the order of the accuracy obtainable. The purpose of this report is to make this information available and show examples of typical results. So far, no work has been done at velocities in excess of 160 feet per second, but with the new instruments, velocity should not be a limiting factor.

IV. TYPES OF HOT-WIRE INSTRUMENTS AND MEASURABLE CHARACTERISTICS OF THE TURBULENCE

All hot-wire instruments considered in this report depend on the rate of heat loss from an electrically heated wire in the wind stream. While some of these instruments are so designed that the rate of heat loss depends on both magnitude and direction of the wind, they may all be regarded as types of hot-wire anemometers. The electrical apparatus is arranged for operation of the wire with constant heating current. This means that the current through the wire may be set at any desired value, but once set is maintained constant either manually or automatically and the wire temperature is allowed to vary as the rate of cooling varies with changes in speed or direction. The resulting change in resistance gives rise to a change in voltage across the wire. Voltage fluctuations, when treated in the manner explained in the following sections, serve to indicate certain characteristics of the turbulence.

The simplest kind of hot-wire anemometer, and the kind that has been used for many years, consists simply of a single wire placed normal to the wind. This kind of instrument, shown in figure 3a responds only to the magnitude of the velocity. Several schemes have been suggested for producing hot-wire instruments with directional characteristics. One such scheme is to place two wires very close together and so obtain a differential heat loss that depends on the direction of the wind. While some investigators havereported success with this scheme, the instruments appear to be difficult to construct. The writers' experience has shown that it is much easier from the standpoint of technique to take advantage of the directional characteristics of a single wire set at an angle to the wind. Such wires may be used singly as shown in figure 3b or in pairs as shown in figures 3c and 3d. When used in pairs the wires are close together, but lie in separate parallel planes. The characteristics of such instruments are treated in section VII, and the method of construction is described in section V. The development and use of hot-wire instruments has been restricted to the types shown in figure 3.

The single wire shown in figure 3a is sensitive to u and is used to measure u'. The single slanting wire shown in figure 3b is sensitive to u and v when lying in the xy-plane and to u and w when lying in the xz-plane, and is used in the xy-plane to measure $\overline{uv}$. It is pointed out that so far all experimental work has been confined to the two-dimensional case in which $\overline{uw}$ is zero. The pair of wires intersecting at about 90° shown in figure 3c may also be used to measure $\overline{uv}$, and when properly constructed, an instrument of this type has certain advantages over one with a single slanting wire. The x-wire arrangement shown in figure 3d differs from figure 3c only by the smaller angle of intersection and is used so as to be sensitive only to v when the wires lie in the xy-plane and to w when the wires lie in the xz-plane. This instrument is used in the respective planes to measure v' and w'.

The measured quantities are therefore u', v', w', and $\overline{uv}$. It is desirable that these values should pertain to a point in the boundary layer. Actually, they are averages over the space occupied by the wires. The wires are made short and the arrangement is made compact so that the space occupied will be small compared to the thickness of the boundary layer. In this connection the advantage of a thick boundary layer is obvious. The x-arrangement with the wires

as close together as practicable is employed in order to place both wires as nearly as possible in a region where the mean velocity will be the same for both.

The turbulent shearing stress τ and the correlation coefficient K are obtained from

$$\tau = -\rho\overline{uv} \tag{1}$$

$$K = \frac{\overline{uv}}{u'v'} \tag{2}$$

So far, no method has been found for the direct measurement of the mixing length l. However, on the assumption of similarity of flow patterns in turbulent exchange, proposed by Von Kármán (reference 1), τ is everywhere proportional to $\rho l^2(dU/dy)^2$; and since l is only a relative measure of the size of the flow pattern, l may include the factor of proportionality and be defined by

$$\tau = \rho l^2(dU/dy)^2 \tag{3}$$

Relation (3) involves the additional assumption that the viscous shearing stress given by $\mu dU/dy$ may be neglected in comparison to the turbulent shearing stress. This assumption is valid everywhere outside of the laminar sublayer. When dU/dy is known from the measured velocity distribution, l may be calculated by means of equations (1) and (3).

It would, of course, be desirable to measure the scale of the turbulence by means of the correlation between like components at different points, as has been done for isotropic turbulence (reference 5). Certain measurements of this sort appear to be possible, say with separate instruments at different points, but at present such measurements are regarded as problems for future development. Only quantities that have actually been measured are to be considered here. These, it is thought, are among the more important quantities needed for the immediate solution of the turbulent boundary-layer problem.

V. NEW DESIGNS OF HOT-WIRE INSTRUMENTS AND METHOD OF CONSTRUCTION

(a) General Features of the New Design

The instruments shown in figure 3 are the types recently developed for boundary-layer investigation. The prongs with the wires attached across the tips are shown by a, b, c, and d. Figure 3e shows a complete instrument with the stem consisting of a 1/8-inch brass rod 5½ inches long by which the instrument is supported on a traversing apparatus, and the flexible leads attached to each prong by which connection is made to long leads running to the electrical equipment outside of the tunnel.

These instruments employ tungsten wires 0.00031 inch in diameter and about 1/16 inch long. The wires were made as short as sensitivity requirements would permit with wire of this diameter. Smaller diameters would make it possible to use shorter lengths, but a diameter of 0.00031 inch appears to be the smallest commercially available in tungsten wire at present. The prongs are about 1/2 inch in length and are made from 0.013-inch phosphor bronze wire. These prongs are flexible and supply spring tension to keep the tungsten wires straight and at a fixed angle with respect to the stem.

The distinctive feature of these instruments is the use of tungsten wire instead of the platinum wire that was always used on older types. Platinum wire has certain advantages over tungsten, such as availability in smaller diameters and higher allowable operating temperatures, but it has very much lower tensile strength and cannot be supported under tension. Platinum wire about 0.0002 inch in diameter, drawn by the Wollaston process, was usually employed. Without tension it was impossible to keep the wires straight and in a fixed orientation, and as a result the calibration of the older instruments could not be maintained. Tungsten wire permits the use of the necessary tension and, in addition, produces a very much more rugged instrument. As mentioned in the introduction, platinum wires could not be used at all in the open-air wind tunnel where it was impossible to keep the air clean and entirely free from flying particles. The two principal difficulties were breakage from collision with solid particles and the accumulation of dirt on the wire.

Breakage rarely occurs with tungsten wire, but the dirt accumulates just the same. However, tungsten wires are sufficiently rugged to permit the removal of dirt by brushing with a small brush.

(b) Method of Attaching Tungsten Wire

The advantages of the superior strength of tungsten wire for application to hot-wire anemometers has been pointed out by Weske in reference 6. However, there has always been one serious drawback to the use of tungsten - namely the difficulty of attaching it to prongs or holders. Whereas platinum wire can be readily soldered with ordinary tin-lead solder, no known solders are entirely satisfactory for tungsten wire. Welding is a possibility, but it is unlikely that the average experimenter will have the skill and equipment required. Weske first called attention to the fact that electroplating the wire with a metal that could be soldered made it possible to use ordinary soldering methods. However, Weske's scheme of plating a thin layer of platinum over the whole wire has the disadvantage of increasing the diameter of the wire and thereby increasing the lag. A variation of the plating scheme was therefore tried with the object of plating the wire only where contact was to be made with the prongs. For this purpose a special copper-plating bath was devised as shown in figure 4. Copper sulphate solution is contained in two wells separated from each other by an air gap. The wire is threaded through the holes in the wells as shown, and solution is then added until the level is slightly above the holes. If the walls are dry on the outside and the holes are small, surface tension prevents leakage. With this arrangement two copper-plated sections are obtained with an unplated section in the middle. The middle section is used as the hot-wire element, and its length is thus definitely defined by the width of the air gap. A microphotograph of a wire processed in this way is shown in figure 4. Any number of hot-wire elements of equal length may be made up by merely pulling another portion of wire into place and repeating the process.

Wires prepared in this way were then attached to prongs by soldering with ordinary tin-lead solder and a flux of zinc chloride solution to produce the instruments shown in figure 3. While a satisfactory mechanical connection was always obtained, the electrical connection was at first unsatisfactory because of an erratic contact resistance. In certain cases there was no evidence of contact resistance for days or possibly

weeks, and then for no accountable reason a resistance suddenly appeared. After much experimentation a technique was found for making satisfactory and lasting connections, which, in essence, amounted to plating slowly enough to get good adhesion between the copper and the tungsten. The thickness of the deposit did not appear to matter, although it was suspected that the differential expansion between copper and tungsten might have a tendency to break the contact if the copper deposit was thick. A clean tungsten surface was obviously to be desired, but no sure method of cleaning was found. Fortunately for the method, contact troubles disappeared when a sufficiently slow plating rate was adopted. The electrolyte used was the same as that ordinarily used in copper plating: 250 grams of crystallized copper sulphate and 75 grams of sulphuric acid per liter of electrolyte. As a precaution against corrosion from the soldering flux, the wires and prongs were washed with a soda solution.

Regardless of whether the plating is thick or thin, the plated and unplated portions are well defined. The copper-plated portions are readily tinned by the solder, and no solder adheres to the bare tungsten. There is, therefore, no difficulty about placing the tips of the prongs at the edge of the copper and thus definitely defining the length of the wire.

(c) Temperature Limitation

The only undesirable property of tungsten wire found so far is its inability to withstand temperatures as high as those withstood by platinum. Tungsten will, of course oxidize in air at yellow heat, but fine tungsten wires apparently deteriorate at considerably lower temperatures. It has been found that 0.00031-inch-diameter wire will withstand temperatures in the neighborhood of 300° C for an indefinite length of time without showing any signs of deterioration or weakening. Above 350° C, the resistance gradually increases with time and rupture finally occurs. These temperatures are averages over wires about 1/16 inch long. Since wires of this length are considerably hotter in the middle than near the ends, the deterioration probably occurs in the middle at some temperature above the average. It follows, therefore, that longer wires with proportionately smaller end effects will withstand higher average temperatures. The instruments shown in figure 3 had adequate sensitivity for the amplification available with wire temperatures no higher than 250° C.

While platinum wire may be run at much higher temperatures, even to the point of glowing brightly, the wire usually lasted longer and maintained its calibration better when the temperatures were less than 400° C.

VI. ELECTRICAL EQUIPMENT

The electrical equipment associated with the hot-wire instruments is fundamentally the same as that described in reference 7. The general scheme always has been to heat the wire with a known constant current and to measure the mean voltage and the fluctuating voltage across the wire. This is known as constant-current operation. Since the publication of reference 7, the hot-wire circuits have been modified by Mr. Mock to include circuits for two hot wires the controls have been modified for greater convenience of operation, and the equipment generally has been made lighter and more portable. The assembled equipment is shown in figure 5, where the three basic units are: the amplifier A, its power supply B, and the control unit C. All units are properly shielded internally and externally to prevent pick-up from stray electric fields. The circuit diagrams for these three units are shown in figures 6, 7, and 8. The circuit diagrams are given here mainly to help the reader to understand the functions of the control unit and the amplifier. For those who may wish to construct such equipment, the diagrams will be useful in conjunction with the detailed treatments given in references 7, 8, 9, and 10. Only those features of the circuits that determine the performance of the hot-wire instruments will be discussed here. It should be remarked that a radically different type of hot-wire circuit described in reference 11, permitting constant-temperature operation, is worthy of consideration, especially for highly turbulent flow where the temperature fluctuations with constant-current operation may on occasions exceed the high-temperature limit for tungsten wire.

(a) Control Unit

The control unit contains, in addition to the controls, the potentiometer and Wheatstone bridge for measuring current, mean voltage, and resistance. The various components are found in the circuit diagram shown in figure 6. The heating current is supplied by storage batteries, requiring from 6 to 12 volts for each wire depending on the current.

For 0.00031-inch diameter tungsten wire the current is usually no greater than 160 milliamperes. Separate batteries are used for each wire. The 12-henry chokes L in each battery circuit provide sufficient impedance to afford constant-current operation during velocity variations associated with turbulence. In more precise terms, the reactance $2\pi fL$ together with the ohmic resistance in the circuit is sufficient to reduce current variations to negligible proportions for all frequencies above the cut-off frequency of the amplifier. For different mean velocities the current must be reset manually by means of rheostats. The 4-dial decade voltage divider is placed in the circuit as potentiometer or bridge, depending on the position of circuit selector No. 2. Circuit selector No. 1 permits the operator to measure the current through either wire, the mean voltage across either wire or the sum or the difference of the voltages across the wires, and the resistance of either wire at air temperature or the sum of the resistances. Another position on selector No. 2 impresses the voltages on the amplifier, individually or the sum or the difference as selected by selector No. 1. When measuring resistance, R12 is thrown in the bridge circuit to make the bridge current sufficiently small to prevent heating of the wires. The leads are always in series with the wires, and correction must always be made for the leads to obtain the resistance of the wires only or the mean voltage across the wires only. An alternating voltage is supplied by an oscillator through the control unit for calibrating the amplifier. This voltage is the drop across R9 and is measured by the thermoelement and microammeter. The various functions of this rather complex control unit will be made clear by tracing the circuits for various positions of the selectors.

(b) Amplifier

Since the voltages may be combined in the control unit when the response of two wires is to be obtained simultaneously, only one amplifier is necessary. The circuit diagram of the amplifier is shown in figure 7. Electrically, this amplifier may be described as a 7-stage capacitance-compensated amplifier. The purpose of compensation is to obtain an amplification increasing with frequency in the same manner as the fluctuating voltage across a hot wire decreases with frequency. As will be shown in section VII, this characteristic of a hot wire, known as lag, may be expressed in terms of a time constant M, which varies with the size of the wire and the operating conditions.

For a harmonic velocity variation of constant amplitude the ratio of the voltage fluctuation across the wire at frequency f to the voltage fluctuation at zero frequency is given by

$$\frac{1}{\sqrt{1 + 4\pi^2 f^2 M^2}}$$

The input to the amplifier therefore decreases as frequency increases, in accordance with the above-mentioned relation. If the input voltage to one of the stages is made proportional to

$$\sqrt{1 + 4\pi^2 f^2 M^2}$$

the final result is an output independent of frequency. Under proper conditions as described in reference 8, this may be done with a load reactance consisting of inductance and resistance or capacitance and resistance. In the present amplifier capacitance and resistance are used as shown under "time constant selector" in the circuit diagram. In this case the time constants are C9 times R12, C8 times R12, and so forth, giving values of M of 0.001, 0.002, 0.003, 0.004, 0.005, and also 0 second. For proper compensation the time constant should be set to the same values as the time constant for the wire. When the time constant for the wire falls between the settings provided, as it usually does, readings must be taken for two settings and the correct result obtained by interpolation.

The design of the amplifier was dictated largely by the impedance requirements for the capacitance type of compensation (reference 8) and by the over-all frequency characteristics desired. The ideal compensated amplifier is one that works in conjunction with a hot wire to give an output truly representative of all frequencies present in turbulent flow. The present amplifier has an error of less than 2 percent between 10 and 2000 cycles per second with the error increasing to 10 percent at 5000 cycles per second. The error below 10 cycles per second has not been experimentally determined, but the amplification begins to drop with decreasing frequency due to the characteristic low-frequency cut-off of resistance-capacity coupling. According to the values of R1 and C1, the output voltage at 1 cycle per second is reduced to about

70 percent of that at frequencies above 10 cycles per second. As shown by Dryden in reference 10, these frequency characteristics are satisfactory for measurements of fluctuations ordinarily encountered in isotropic turbulence. The frequency distribution in turbulent boundary layers is not known and probably varies in different parts of the layer. It is believed, however, that the amplifier is just as satisfactory for measurements in turbulent boundary layers as in fields of isotropic turbulence if the proportion of the turbulent energy lying below 10 cycles per second is the same in the two cases.

Other features of the amplifier are evident in the circuit diagram. The gain control permits the amplification to be varied over wide limits. A phase inverter and balanced output are used to prevent direct current from flowing through the thermoelements. Thus only the alternating current produced by the fluctuating hot-wire voltage is read on the output meter. The amplifier is calibrated by reading the output meter with known input voltages. An unknown mean-square input voltage may then be determined from the output meter reading. The "eye" (6E5) gives a rough indication of the reading to be expected and is used to enable the operator to judge whether he is likely to burn out the fuse, and possibly the thermoelements, when depressing the key.

(c) Power Supply

By means of the dual power supply shown in figure 8, the amplifier is operated completely on 115-volt, 60-cycle current. The power-supply circuit is conventional except for the voltage-regulator circuits lying to the right of the filter circuits. The voltage regulator serves two purposes. First it holds the output voltage practically constant regardless of reasonable changes in load and input voltage to the unit. Secondly, because of its regulating action, it acts as an efficient filter circuit, and also causes the power supply to appear to have a very low internal resistance. Since the requirements to be met by a satisfactory power supply are treated in detail in reference 7, no further discussion is given here.

VII. CHARACTERISTICS OF HOT WIRES AND THEORY OF HOT-WIRE MEASUREMENTS

The relation between the air velocity normal to a heated wire and the rate of heat loss as given by King (reference 12) is

$$\frac{h}{\bar{T} - T_a} = D_1 + F_1 \sqrt{U} \qquad (4)$$

where the terms D_1 and F_1 depend on the thermal conductivity, density, and specific heat of the air and the dimensions of the wire as shown in reference 12. Owing to the methods of using hot wires in boundary-layer investigations, D_1 and F_1 may be regarded as constants. When the wire is heated by an electric current i, the heat is supplied at the rate i^2R, where R is the resistance of the wire at temperature $\bar{T}$. The temperature head $\bar{T} - T_a$ is

$$\bar{T} - T_a = \frac{R - R_a}{R_0 \alpha}$$

$\alpha = \frac{1}{R_0} \cdot \frac{R}{T}$

Under equilibrium conditions the rate of heat loss must be equal to the rate at which heat is supplied, and equation (4) may be written

$$\frac{i^2 R(R_0 \alpha)}{R - R_a} = D_1 + F_1 \sqrt{U} \qquad (5)$$

Equation (5) is the usual form of the relation used in hot-wire anemometry. Equation (5) is found to hold true over a wide range of velocities.

In the expressions to follow it will be convenient to disregard the distinction between mean quantities and instantaneous quantities. In the few cases where a distinction is necessary, appropriate symbols will be used. The usual distinction between mean quantities and fluctuations still will be made.

As previously mentioned, the control unit has been designed for constant-current operation, which means that i

is constant. For convenience, the constant terms in equation (5) are included in the constants on the right, and the equation is written

$$\frac{R}{R - R_a} = D + F\sqrt{U} \qquad (6)$$

Equation (6) expresses the relation between $\frac{R}{R - R_a}$ and U for a given wire heated with a given constant current. The voltage E across the wire is simply iR, and is the quantity usually observed rather than R. The observations are usually expressed in terms of $\frac{R}{R - R_a}$ because of the linear relation between this quantity and $\sqrt{U}$.

Equation (6) is found to hold true regardless of the angle between the axis of the wire and the wind. The constant F, however, depends on the angle. When the voltage is observed for various angles between the axis of the wire and the wind at fixed values of U, E is found to vary as shown in figure 9. When $\frac{R}{R - R_a}$ is calculated from the voltage and the measured R_a and is plotted against φ, the curves shown in figure 10 are obtained. If as seems logical, the heat loss is a function of the component of the velocity normal to the wire, the general form of equation (6) should be

$$\frac{R}{R - R_a} = D + F\sqrt{U \sin \varphi} \qquad (7)$$

In order to test this relation, $\frac{R}{R - R_a}$ is plotted against $\sqrt{U \sin \varphi}$ as shown in figure 11. If equation (7) is valid, all points should lie on a single straight line. The line is reasonably straight above $\sqrt{U \sin \varphi} = 4$. The fact that not all the points lie on the same line is attributed to an accumulation of dirt on the wire as the run progressed. Equation (7) therefore may be regarded as a reasonably good approximation over the linear range. Since equation (6) is valid over a wide range of velocities, the linear range in figure 11

depends on the value of φ. If φ lies between 20° and 90°, the curve is linear for all values of U sin φ. It should be noted that, when φ is constant, the curve is always linear regardless of the value of φ, for then equation (7) reduces to the form of equation (6) with $F\sqrt{\sin\varphi}$ taking the place of the constant F in equation (6). However, separate linear curves are obtained for each value of φ below 20°.

When the velocity varies either in magnitude or direction, the voltage across the wire varies. The instantaneous velocities may be regarded as a superposition of u, v, and w, on the velocity U. Since v and w are by definition at right angles to U, these two fluctuations, if they are small compared to U, produce only a variation in the local direction of the stream. The angle variation, expressed in radians, for a wire lying in the xy-plane is v/U and for a wire lying in the xz-plane is w/U. Thus

$$\left.\begin{aligned}(\text{xy-plane})\quad \Delta\varphi &= \frac{v}{U}\\ (\text{xz-plane})\quad \Delta\varphi &= \frac{w}{U}\end{aligned}\right\} \qquad (8)$$

It is assumed that u, v, and w are small compared to U, and therefore that the voltage fluctuations associated with u, v, and w are proportional to u, v, and w and may be expressed by

$$\left.\begin{aligned}e_1 &= Au\\ e_2 &= Bv\\ e_3 &= Pw\end{aligned}\right\} \qquad (9)$$

The corresponding root-mean-square values are written

$$\left.\begin{aligned}e_1' &= \sqrt{A^2}u'\\ e_2' &= \sqrt{B^2}v'\\ e' &= \sqrt{B^2}w'\end{aligned}\right\} \qquad (10)$$

In equations (9) and (10) the voltages are assumed to be the

voltages properly compensated for the lag of wire: that is, they are determined from the output of a properly compensated amplifier. When proper compensation is used; A and B may be evaluated by the aid of equation (7). In other words, compensation for the lag of the wire makes it possible to apply equilibrium relations even though the equilibrum condition assumed in equations (5), (6), and (7) may not actually exist.

Inasmuch as relations (9) are assumed, it is permissible to regard the fluctuating voltages, angles, and velocities, represented by e, $\Delta\varphi$, u, v, and w, respectively, as differentials and evaluate A and B by differentiating equation (7). If dE is regarded as e, dU as u, and $Ud\varphi$ as v or w in equations (8) and (9),

$$A = \frac{dE}{dU} \quad , \qquad B = \frac{dE}{Ud\varphi}$$

Differentiating (7) with respect to U, regarding φ as constant yields,

$$\frac{dR}{dU}\left(-\frac{R_a}{(R-R_a)^2}\right) = \frac{F\sqrt{\sin\varphi}}{2\sqrt{U}}$$

and since $dE = idR$

$$\frac{dE}{dU}\left(-\frac{R_a}{(R-R_a)^2}\right) = \frac{i\,F\sqrt{\sin\varphi}}{2\sqrt{U}}$$

and

$$A = -\frac{i\,F\sqrt{\sin\varphi}}{2\sqrt{U}}\,\frac{(R-R_a)^2}{R_a} \qquad (11)$$

Differentiating (7) with respect to φ, regarding U as constant yields

$$\frac{dR}{d\varphi}\left(-\frac{R_a}{(R-R_a)^2}\right) = \frac{F\sqrt{U}\cos\varphi}{2\sqrt{\sin\varphi}}$$

$$\frac{dE}{U\,d\varphi}\left(-\frac{R_a}{(R-R_a)^2}\right) = \frac{i\,F\cos\varphi}{2\sqrt{U\sin\varphi}}$$

$$B = -\frac{iF\ \cos\varphi}{2\sqrt{U\ \sin\varphi}}\ \frac{(R-R_a)^2}{R_a} \qquad (12)$$

The fact that A and B are negative means simply that the voltages in equations (9) decrease as u, v, and w increase.

The method of evaluating the constants A and B and the manner in which they are used will be considered in connection with each of the quantities to be determined. The purpose of the different arrangements of wires shown in figure 3 is to obtain instruments that will measure one component at a time; for example, measure u' without contamination from $\overline{uv}$, v', and w', or measure v' while excluding u', $\overline{uv}$, and w', and so forth. This can be done more easily in some cases than in others, and in all cases the ideal can be approached only when u, v, and w become small with respect to U. Regardless of the type of instrument, the separation of components is possible only insofar as variations in φ are independent of u and variations in U are independent of v and w. This again requires that u, v, and w be small compared to U.

(a) Determination of u'

For the measurement of u' the wire is placed normal to the wind and parallel to the surface producing the boundary layer. The angle φ is then 90° and A and B as given by equations (11) and (12) become

$$\left.\begin{aligned} A &= -\frac{i\,F}{2\sqrt{U}}\ \frac{(R-R_a)^2}{R_a} \\ B &= 0 \end{aligned}\right\} \qquad (13)$$

Thus according to equations (10)

$$e_1' = -\frac{i\,F}{2\sqrt{U}}\ \frac{(R-R_a)^2}{R_a}\ u' \qquad (14)$$

and e_2' and e_3' are zero. The relations show that this instrument is sensitive to u and insensitive to v and w.

Solving (14) for u' and dividing by U gives

$$\frac{u'}{U} = \frac{2 R_a e_1'}{i F \sqrt{U(R-R_a)}} \qquad (15)$$

All quantities on the right of equation (15), with the exception of F, are determined at each point where u'/U is being measured. The constant F is determined for the particular wire used by placing the instrument in the free stream and measuring the mean voltage E at several values of the velocity U at the location of the wire. The quantity $\frac{R}{R-R_a}$ is then calculated and plotted against U to obtain a calibration curve as shown in figure 12. The slope of this curve is F, since $\varphi = 90°$. The current i must not only be constant during a run, but must be the same for the calibration as for the determination of u'/U.

It is well to see how, and to what extent, a single wire normal to the wind with its axis in the xz-plane responds to u and not to v and w. Since the wire has cylindrical symmetry, the only way in which v can change the rate of heat loss is through changes in the resultant velocity by vector addition with U. The error in a measurement of u'/U arising from v is small until v/U becomes quite large, and when this is the case, the type of error discussed in section IX is so large by comparison that the error arising from v becomes insignificant. The w-fluctuations also change the resultant velocity, but do not change the normal component. Since it has been shown that the heat loss depends only on the normal component, no error arises from w regardless of the size of w/U.

(b) Determination of Turbulent Shearing Stress.

According to equation (1) the determination of turbulent shearing stress involves the measurement of $\overline{uv}$. For this purpose, use is made of either the single slanting wire shown in figure 3b, making an angle φ of about $45°$ to the wind, or the x-wires shown in figure 3c, set approximately $90°$ to each other and each making about $45°$ to the wind. The manner in which these wires are used is illustrated in figure 13. Consider first the single wire, first in position

I and then rotated 180° about an axis in line with the wind to position II. Figure 9 shows that the voltage decreases as U and φ increase. Therefore in position I, +u and +v, as defined in figure 13, both decrease the voltage; and the resultant voltage change is the sum of e_1 and e_2 in accordance with equations (9). In position II +u decreases the voltage while +v increases the voltage, and the resultant voltage is the difference between e_1 and e_2. As previously explained, the mean-square of the resultant voltage fluctuation may be determined from the output meter reading of the compensated amplifier. If the mean-square resultant for position I is denoted by a and the mean-square resultant for position II is denoted by b,

$$a = \overline{(-e_1 - e_2)^2} \quad , \quad b = \overline{(-e_1+e_2)^2}$$

From equations (9)

$$a = \overline{(-A_I u - B_I v)^2} = A_I^2\overline{u^2}+2A_IB_I\overline{uv}+B_I\overline{v^2} \tag{16}$$

$$b = \overline{(-A_{II}u + B_{II}v)^2} = A_{II}^2\overline{u^2} -2A_{II}\,B_{II}\overline{uv}+B_{II}\overline{v^2} \tag{17}$$

where subscripts I and II refer to the value of the constants for positions I and II, respectively.

In using the wire, a and b are determined in positions I and II, care being taken to make the 180° rotation from one position to the other about an axis through the center of the wire and along the average wind direction. When rotated in this way, there is no change in the average value of φ. If, in addition, the average condition of the boundary layer remains the same, equations (11) and (12) show that $A_I = A_{II} = A$ and $B_I = B_{II} = B$. Under these conditions the sum and difference of equations (16) and (17) become

$$a + b = 2(A^2\overline{u^2} + B^2\overline{v^2}) \tag{18}$$

$$a - b = 4\,AB\,\overline{uv} \tag{19}$$

From equations (1) and (19) is found

$$\tau = - \frac{\rho (a-b)}{4 AB} \qquad (20)$$

where, according to equations (11) and (12),

$$AB = \frac{i^2 F^2 (R-R_a)^4 \cos\varphi}{4U R_a^2} \qquad (21)$$

All the quantities on the right of equations (20) and (21), except φ and F, are determined at each point where τ is being determined. According to equation (7), F is the slope of the straight portion of the curve in figure 11, and F is determined from calibration curves of this kind. The angle φ may be determined by plotting $R/R-R_a$ against $\sqrt{U}$, when the wire is set at the proper angle, and, finding the slope of the curve which is equal to $F \sqrt{\sin\varphi}$.

As mentioned above, the x-wire arrangement may be used in place of the single wire for the measurement of shearing stress. If the wires are now labeled I and II as shown in figure 13, the same relations apply as for positions I and II. The 180° rotation is unnecessary; but in order for the conditions $A_I = A_{II} = A$ and $B_I = B_{II} = B$ to apply, the wires must be identical and each must subtend the same angle to the wind. When the wires are prepared by the electroplating method described in section V, it is not difficult to obtain matched wires. Calibration will show whether the wires are sufficiently well matched to be usable, and equal voltages across the wires will indicate the proper setting for the instrument to place the wires I and II at equal angles to the wind. The angle φ is half the angle subtended by the wires and may be determined by direct measurement.

In the earlier type of instrument using platinum wires it was difficult to obtain two wires sufficiently alike to use the x-wire for shearing stress, and consequently the early measurements were all made with single slanting wires. The 180° rotation of the wire is a troublesome feature of this method, not so much because of mechanical complications,

but because of the difficulty of passing the axis of rotation through the midpoint of the wire. It is seldom possible to avoid some amount of displacement to and from the surface in rotating from one position to the other. This difficulty is avoided with the x-wires, and the instrument support system may be simplified by the elimination of a rotation mechanism. The disadvantages of the x-wire are that the instrument is more difficult to construct even when tungsten wires are used and two wires must hold their calibration instead of one. An accident to either wire puts the instrument out of service.

(c) Determination of Correlation Coefficient

The correlation coefficient K is defined by equation (2). Since K involves $\overline{uv}$, u' and v', its evaluation depends on the measurements of these three quantities. There are in fact three ways to evaluate K, all three being interrelated but involving u' and v' in different ways. Because of experimental errors, the three methods, that should yield identical results, will in general produce three somewhat different values of K. It is therefore advisable to label them K_1, K_2, and K_3 to correspond to the first, second, and third method.

The first method depends mainly on the results obtained in the measurement of shearing stress. Equation (18) is solved for v' and equation (19) is solved for $\overline{uv}$. Then it follows that

$$v' = \sqrt{\frac{a+b}{2B^2} - \frac{A^2}{B^2}\,u'^2} \tag{22}$$

$$\overline{uv} = \frac{a-b}{4AB} \tag{23}$$

where by definition u' and v' stand for $\sqrt{\overline{u^2}}$ and $\sqrt{\overline{v^2}}$. If (22) is multiplied by u' and (23) divided by the result, there is obtained

$$K_1 = \frac{\overline{uv}}{u'v'} = \frac{\frac{a-b}{4AB}}{u'\sqrt{\frac{a+b}{2B^2} - \frac{A^2}{B^2}\,u'^2}} \tag{24}$$

Thus K_1 may be calculated from the data taken in connection with a determination of shearing stress together with an independently measured value of u'.

The second expression for the correlation coefficient is obtained by dividing equation (19) by (18) and solving for $\overline{uv}/u'v'$. It is found that

$$K_2 = \left(\frac{a-b}{a+b}\right) \frac{\frac{A^2}{B^2}\frac{u'}{v'} + \frac{v'}{u'}}{2\frac{A}{B}} \qquad (25)$$

Here the data taken in connection with a determination of shearing stress are used in such a way that only the ratio of the constants A and B and the ratio of u' to v' enter into the expression for the correlation coefficient. In this case both u' and v' must be determined by independent measurement.

Finally, by solving equation (19) for $\overline{uv}$ and dividing by u' and v' it is found that

$$K_3 = \frac{a - b}{4AB\,u'v'} \qquad (26)$$

or by equation (20)

$$K_3 = -\frac{\tau}{\rho u'v'} \qquad (27)$$

As shown by equation (27), the third method amounts simply to using the measured shearing stress and the independently measured u' and v'.

Calculation of the correlation coefficient by all three methods affords a check on the accuracy of the measurements. Complete agreement can scarcely be expected, and there is probably a best value depending on the accuracy with which the various terms are known. As noted, K_2 involve only the ratios u'/v', and A/B. According to equations (11) and (12)

$$\frac{A}{B} = \tan\varphi \qquad (28)$$

and therefore A/B is less subject to error than A and B separately. When $\varphi = 45^\circ$, the percentage error in $\tan\varphi$ is a minimum for an error in φ. Furthermore, according to equation (25) no error in K_2 results from an error in u'/v' when $A/B = v'/u'$. Since v'/u' is not greatly different from unity, the optimum conditions appear to be

$$A/B = \tan\varphi = 1, \qquad \varphi = 45^\circ$$

It is concluded therefore that K_2 is probably the best value of the correlation coefficient. On the other hand, only K_3 will be consistent with the measured values of τ, u' and v'. If the difference between K_2 and K_3 is significant, the least certain of the quantities τ, u', and v' should be derived from equation (27) using K_2. In this way the best consistent set of results will be obtained.

So far it has been assumed that a slanting wire or an x-wire in the xy-plane is insensitive to w. On the average there is no flow across the xy-plane by definition of this plane. At any instant, however, the flow makes an angle with the xy-plane given by w/U. In order to see how well the assumption is justified it is necessary to find out how much of a change w/U produces in the angle between the wire and the wind. If the angle w/U is denoted by $\Delta\psi$ and the instantaneous angle between the wire and the wind by φ_i, it is found from geometrical relations that

$$\sin\varphi_i = \cos\varphi \sqrt{\sin^2\Delta\psi + \tan^2\varphi} \qquad (29)$$

It is seen from equation (29), for example when $\varphi = 45^\circ$, that $\Delta\psi$ must exceed 0.175 radian or 10° before $\varphi_i - \varphi$ $(= \Delta\varphi)$ is greater than 1°. The smallness of the effect on φ is the reason for assuming that wires in the xy-plane are insensitive to w. Just how large w/U may become before this assumption is no longer justified is difficult to estimate because of the distorted nature of the voltage fluctuation resulting from w.

In two-dimensional flow there is no error from w in the measured shearing stress because of the fact that w is not correlated with u or v. Whether or not there is an error in the measured correlation coefficient depends on

the effect of v and w in the measurement of u' and of u and w in a measurement of v'. It has already been shown that the effect of v and w is negligible in a measurement of u'. The effect of u and w in the measurement of v' will be considered presently.

(d) Determination of v' and w'

As far as the theory is concerned, there is no difference between the measurement of v' and w'. The x-wire instrument is used in both cases — in the xy-plane for v' and in the xz-plane for w'. Therefore the relations for v' will be derived, and the same relations hold true for w'.

Figure 13 illustrates the position of the wires for a measurement of v'. Whereas for the measurement of shearing stress, the mean-square voltages, denoted by a and b, were determined for the wires separately, now the mean-square resultant voltage is determined for the pair. In other words, the voltage across the pair is impressed on the amplifier and only the resultant is measured. This is illustrated as follows: Referring to figure 13, let $-e_1 - e_2$, as defined by equation (9), be the voltage across wire I and $-e_1 + e_2$ be the voltage across wire II. The mean-square resultant voltage when added is

$$\overline{e_a^2} = \overline{\left[(-e_1-e_2)_I + (-e_1+e_2)_{II}\right]^2} \tag{30}$$

and when subtracted is

$$\overline{e_b^2} = \overline{\left[(-e_1-e_2)_I - (-e_1+e_2)_{II}\right]^2} \tag{31}$$

According to equations (9), using constants A_I and B_I for wire I and A_{II} and B_{II} for wire II, equations (30) and (31) become

$$\overline{e_a^2} = \overline{(-A_I u - B_I v - A_{II} u + B_{II} v)^2}$$

$$\overline{e_a^2} = A_I^2\overline{u^2} + B_I^2\overline{v^2} + A_{II}^2\overline{u^2} + B_{II}^2\overline{v^2} + 2A_IB_I\overline{uv} + 2A_IA_{II}\overline{u^2}$$
$$-2A_IB_{II}\overline{uv} + 2B_IA_{II}\overline{uv} - 2B_IB_{II}\overline{v^2} - 2A_{II}B_{II}\overline{uv} \quad (32)$$

$$\overline{e_b^2} = \overline{(-A_I u - B_I v + A_{II} u - B_{II} v)^2}$$

$$\overline{e_b^2} = A_I^2\overline{u^2} + B_I^2\overline{v^2} + A_{II}^2\overline{u^2} + B_{II}^2\overline{v^2} + 2A_IB_I\overline{uv} - 2A_IA_{II}\overline{u^2} \quad (33)$$
$$+2A_IB_{II}\overline{uv} - 2B_IA_{II}\overline{uv} + 2B_IB_{II}\overline{v^2} - 2A_{II}B_{II}\overline{uv}$$

When $A_I = A_{II} = A$ and $B_I = B_{II} = B$, (32) and (33) reduce to

$$\overline{e_a^2} = 4A^2\overline{u^2} \quad (34)$$

$$\overline{e_b^2} = 4B^2\overline{v^2} \quad (35)$$

Thus, in accordance with equations (11) and (12), when the two wires are identical and each subtends the same angle to the wind, $\overline{e_a^2}$ is a measure of $\overline{u^2}$ only and $\overline{e_b^2}$ is a measure of $\overline{v^2}$. When the two wires are not identical or do not subtend the same angle to the wind, the result is a mixture of $\overline{u^2}$, $\overline{v^2}$, and $\overline{uv}$. Equation (34) shows that the

x-wire instrument may be used to measure u', but due to the possibility of obtaining a mixture of components, the single wire normal to the wind is preferable. In order to lessen the possibility of a mixture of components in the measurement of v', B is made larger than A; that is, the angle φ is made less than 45°.

While the foregoing relations are useful to illustrate how the characteristics of individual wires can be combined to produce an instrument sensitive to v, these relations, as such, are not used to determine v'. In practice it is unnecessary, as well as too laborious to determine the constants B for the individual wires. Instead, the sum and the difference of the mean voltage across the pair of wires are determined as a function of velocity and angle, and in this way a calibration curve is obtained for determining v'/U from the root-mean-square voltage fluctuation directly. The basis for this procedure is illustrated by the performance characteristics given in figures 14 and 15.

Figure 14 shows the mean voltages as measured on the potentiometer for wires I and II as a function of angle between the stem of the instrument and the wind at a velocity of 124 feet per second. The difference voltage E_b, also measured on the potentiometer, is shown by the broken curve. It is seen that while the curves for the wires individually are far from linear in the neighborhood of zero angle, E_b is practically linear with angle over a range of 30°. The reciprocal of the slope indicates the sensitivity of the pair of wires to v. When the slope is expressed in terms of volts per radian and is denoted by ΔE_b there exists the simple relation

$$\frac{v'}{U} = \frac{\sqrt{\overline{e_b^2}}}{\Delta E_b} \tag{36}$$

where $\sqrt{\overline{e_b^2}}$ is determined from the compensated output reading of the amplifier and ΔE_b is determined by calibration. The calibration consists of determining ΔE_b at various velocities. A calibration curve shown in figure 15 is obtained by plotting ΔE_b against $R/R-R_a$ for the pair of wires. This affords a convenient means for obtaining ΔE_b without having to know the mean velocity at each point in the boundary layer.

In use, the proper angle for setting the instrument is found by making E_b zero regardless of the angle between the stem of the instrument and the wind. If the stem is out of alinement with the wind, for example, 5° as shown in figure 14, the two wires are not set at the same angle with respect to the stem or the wires are imperfectly matched.

The voltage fluctuation produced by w is removed as a potential source of error in the measurement of v' because the subtraction indicated in equation (31) is made before squaring. In other words, if equation (29) were used to find $\Delta\varphi$, a positive $\Delta\varphi$ would be found for both wires, and there would be no net effect on the difference voltage.

The effect of u in a measurement of v' may be found quite simply by considering that φ is assumed to be v/U when actually it is $\frac{v}{U\pm u}$. Then actually $v/U\pm u$ is being measured or approximately

$$\frac{v}{U}\left(1 \mp \frac{u}{U}\right)$$

when $\frac{u}{U}$ is small compared to 1. The root-mean-square value of this expression is

$$\frac{v'}{U}\left(1 + 1/2\,\frac{\overline{u^2}}{U^2}\right) \quad \text{approximately} \qquad (37)$$

From this expression the error in v'/U may be found. If, for example, u'/U is 0.3, the measured v'/U is too high by 4½ percent.

(e) Hot-Wire Lag

Because of the heat capacity of the wire, a certain time is required for the wire temperature to reach equilibrium after a change has occurred in the rate of heat loss accompanying a change in magnitude or direction of the wind. If $T_e - \overline{T}$ is small compared to $\overline{T} - T_a$, the relation between the instantaneous temperature T and the equilibrium temperature T_e is given by

$$M \frac{dT}{dt} = T_e - T \tag{38}$$

where M is termed "the time constant." The solution of (38) consists of a transient term $\exp\left(-\frac{t}{M}\right)$ and a periodic term, if T_e is periodic. Since the transient term soon becomes negligible, only the periodic term will be considered. As shown in reference 9, if the temperature variation is periodic with frequency f, the temperature variations and corresponding voltage variations are reduced in amplitude below that for zero frequency by the factor

$$\frac{1}{\sqrt{1 + 4\pi^2 f^2 M^2}} \tag{39}$$

and lag in phase by the angle

$$\gamma = \tan^{-1} 2\pi f M \tag{40}$$

With regard to the irregular wave form of turbulent fluctuations, which results from a superposition of many frequencies, (39) and (40) mean that the voltage fluctuation from each component frequency is reduced in the ratio of 1 to $\sqrt{1 + 4\pi^2 f^2 M^2}$ and lags in phase by the angle γ. Consequently the wave form of the voltage across the wire fails to reproduce the wave form of the turbulence.

The expression for M is derived in reference 9 for the case where the heating current is constant and is given as

$$M = \frac{4.18\ ms\ (R - R_a)}{i^2\ R_a\ R_o \alpha} \tag{41}$$

where

m mass of the wire

s specific heat of the material of the wire

4.18 mechanical equivalent of heat, joules per calorie

In reference 10 an expression for M is derived for the more general case in which the heating current varies with the resistance of the wire. However, only constant-current operation and therefore equation (41) will be considered here.

As a matter of convenience, the terms on the right of equation (41) are separated into those that depend on the wire and those that depend on the operating conditions. Equation (41) then becomes

$$M = M_c \left(\frac{R - R_a}{i^2 R_a} \right) \tag{42}$$

where M_c depends on the wire and $\frac{R - R_a}{i^2 R_a}$ depends on operating conditions. According to equation (41) M_c is given by

$$M_c = \frac{4.18\ ms}{R_o\ \alpha} = \frac{4.18\ \pi^2\ r^4\ \rho_1 s}{\sigma_o\ \alpha} \tag{43}$$

where

r radius of the wire

ρ_1 density of material of the wire

σ_o resistivity of the material of the wire at 0° C

If M_c is known, M may be calculated by equation (42) for any working condition. While it is possible in principle to calculate M_c by equation (43) from the radius of the wire and the properties of the material, there are two reasons why it is not feasible to do so. First, it is difficult to measure r with the accuracy required by the fourth-power relation; and second, equation (41) is not strictly valid for short wires because of end effects. The expression M_c is therefore determined by measuring the lag of samples of the wire under known operating conditions on an apparatus which vibrates the hot wire in a steady air stream at various known frequencies. Several experimental values of M_c for tungsten wire with a nominal diameter of 0.00031 inch are as follows:

Wire length (mm)	M_c
1.1	504×10^{-7}
2.5	389
3	366

The value of M_c calculated by equation (43) is 263×10^{-7}.

It will be observed that the experimentally determined M_c increases with decreasing wire length; whereas, according to equation (43), M_c should be independent of wire length. This effect is due to the conduction of heat from the ends of the wire to the prongs, which is not taken into account in the derivation of equation (41). Because of this additional heat loss, a greater current is required to produce a given temperature rise than would be required otherwise. This leads to the conclusion that the principal effect of wire length appears in the quantity $\frac{R - R_a}{i^2 R_a}$, used to calculate M_c in a lag determination; and this conclusion is borne out by the experimental results which show that $\frac{R - R_a}{i^2 R_a}$ changes with wire length rather than M itself.

When the wire is used to measure turbulence, $\frac{R - R_a}{i^2 R_a}$ is found for each determination, and M is calculated by equation (42) with the value of M_c for the wire length used. The calculated time constant is found to be about the same for short wires as for long wires. Unfortunately this does not mean that the procedure is entirely correct, and it is thought that end effects introduce some uncertainty in the evaluation of the time constant. Since the uncertainty increases with decreasing length-diameter ratio, wire of 0.00031-inch diameter is not regarded as satisfactory in lengths less than about 1.5 millimeters.

In most applications M is usually between 0.001 and 0.002 second. This is well within the range of time constants provided in the amplifier.

In cases where the sum or difference of instantaneous voltages is taken, as in the determination of v' and w', it is important that both wires have the same time constant in order that there shall be no difference in phase introduced. This is another reason for having the wires as nearly identical as possible and operated at the same mean angle and velocity.

VIII. APPLICATION OF HOT-WIRE INSTRUMENTS AND RESULTS

Following the development and study of new instruments and methods, measurements of u', v', w', and $\overline{uv}$ were made in the turbulent boundary layer along the wall shown in figures 1 and 2. The results obtained so far are far from being sufficiently complete to make a significant contribution to turbulent boundary-layer theory. They are given here mainly as examples of the kind of results obtainable.

Prior to undertaking work with hot-wire instruments, the pressure distribution along the surface was measured and the position of the separation point was determined. A certain amount of preliminary work had to be done to obtain two-dimensional flow over the after portion of the wall and to obtain a straight and well-defined line of separation. The final pressure distribution and separation point at a Reynolds number RN of 15.3 million is shown in figure 16. Attention is called to the region of adverse pressure gradient near the leading edge and to the occurrence of transition therein. This condition resulted from the high effective angle of attack and the small radius of curvature of the leading edge. The turbulence of the free stream was found to be closely isotropic with an intensity of about 1/2 percent.

Mean velocity distributions through the boundary layer were determined at the same Reynolds number by traversing normal to the surface with a small pitot-static tube mounted on the traversing apparatus and support system shown in figure 1. From such distributions, obtained at many stations along the surface, δ, δ^*, θ, and H were found.

The velocity distributions showed certain anomalies near the separation point that are believed to be due to an effect of turbulence on the pitot tube. Effects of this sort appear

in the results of other investigators (reference 13). For this reason it is planned to redetermine some of the velocity distributions at the same time u' measurements are made, since the same hot-wire instrument serves both purposes. The velocity distributions determined so far by the hot wire are shown in figure 17. The velocity distributions are an important adjunct to turbulence data for a number of purposes, one being to calculate mixing length by equation (3).

The results that demonstrate the application of hot-wire instruments are given in figures 19, 20, 21, and 22. The mean velocity contours and the boundary-layer thickness, shown in figure 18, are included here along with figures 16 and 17 to show the kind of boundary layer in which the turbulence measurements were made. The measurements were made at RN = 15.3 million. All these curves were obtained by taking observations at various distances from the surface with the traversing device shown in figure 1. A description of this device will be omitted here, partly because the manner of traversing is incidental to the investigation and partly because the remote-control feature of the device has not proved to be entirely satisfactory for hot-wire work. However, the support system and traversing device shown in figure 1 satisfied an important condition that must be met by any system - namely, that it should not alter the condition of the boundary layer at the position of the hot wire. It is remarked that complete remote control is attended with considerable difficulty due to the requirement that the instruments must be kept in proper alinement with the mean wind in the measurement of v', $\overline{uv}$, and w'. Traversing is therefore a matter that must be worked out to meet particular needs.

Figure 19 shows the distribution of u'/U_1, v'/U_1, and w'/U_1 through the boundary layer at $x = 17\frac{1}{2}$ feet. Figure 20 gives the distribution of friction coefficient c_f for the same position. The friction coefficient is obtained from the shearing stress by the following relation:

$$c_f = \frac{\tau}{1/2\ \rho\ U_1^2} = \frac{2\ \overline{uv}}{U_1^2}$$

The local skin friction coefficient $\tau_0/1/2\rho U_1^2$, estimated from the momentum equation (reference 13) is indicated in the figure. The limits indicate the uncertainty in the local skin

friction at this point. Theoretically, the turbulent shearing stress should decrease in the laminar sublayer and actually fall to zero at the surface. Beyond the laminar sublayer but still close to the surface the turbulent shearing stress may be expected to agree with τ_0. This appears to be the case, since the points nearest the surface are well outside of the laminar sublayer. The correlation coefficients calculated by the three different methods (equations (24), (25), and (27)) are given in figure 21. Coefficients K_1 and K_2 agree, but K_3 is about 17 percent above the other two. This difference, which indicates experimental error, has not yet been accounted for. More observations are necessary before it is possible to decide which of the quantities $\overline{uv}$, u', or v' is least certain and thereby make use of the procedure suggested in section VII for obtaining the best consistent set of results.

Figure 22 shows the distribution of u'/U at several stations in the region of adverse pressure gradient. It will be noted that the ordinates here are the ratio of u' to the mean local velocity instead of the mean velocity at the outer edge of the layer. This method of presenting the results is useful when it is desirable to know whether or not the fluctuations are small compared to the mean local velocity. This subject will be considered in the following section. Figure 22 shows that u'/U increases progressively as x increases. No turbulence measurements have yet been made beyond $x = 22$ feet.

IX. ERRORS WHEN FLUCTUATIONS ARE NOT SMALL

It will be recalled that u, v, w small compared to U was a basic assumption in the development of the equations in section VII. The results in figure 22 may well raise doubts about the smallness of these quantities in a turbulent boundary layer. Beyond a doubt u'/U will continue to increase as the separation point at $x_s = 25.7$ feet is approached, and just how high the value will go is not known. The components v'/U and w'/U and the shearing stress have been determined only at $x = 17\frac{1}{2}$ feet, but it is reasonable to assume that these too will increase with x. The questions are then, how large may u'/U, v'/U, and w'/U become before the fluctuations may no longer be considered small compared to U, and how does the error depend on the size of these quantities?

Unfortunately the answers to these questions are not

easily obtained. When the fluctuations are no longer small, errors arise from the interaction of components, improper compensation for lag, and the nonlinearity of the voltage–velocity curve and the voltage–angle curve for a hot wire operated with constant heating current. The latter concerns the errors in A and B resulting from the assumption that u, v, and w are infinitesimals. When the several kinds of errors are considered, it is found that errors in A and B are probably the largest and therefore deserve first consideration.

Since the wave form of turbulent fluctuations is irregular and jagged, and qualitatively has the appearance of complete randomness, an accurate estimate of the errors in A and B seems to be impossible. A crude method is to assume sinusoidal fluctuations and to find A from experimental voltage–velocity curves and B from experimental voltage–angle curves with the relations for A and B given by

$$A = \frac{\Delta E_{max}}{\Delta U_{max}} \qquad B = \frac{\Delta E_{max}}{U \Delta \varphi_{max}}$$

The ratios A and B are determined by arbitrarily assigning larger and larger increments to ΔU_{max} and to $\Delta \varphi_{max}$ about a point on their respective curves and determining the corresponding ΔE_{max}. For a sine wave

$$\Delta U_{max} = \sqrt{2}\, u', \qquad U \Delta \varphi_{max} = \sqrt{2}\, v' = \sqrt{2}\, w'$$

The values of A and B found in this way are the correct ones for sinusoidal variations in ΔU and $\Delta \varphi$, at least until ΔU_{max} and $\Delta \varphi_{max}$ become so large that the voltage wave is distorted by a significant amount by the nonlinearity of the curves. Obviously, the weakness in this method is the inference that there exist relations like

$$u_{max} = \sqrt{2}\, u', \qquad v_{max} = \sqrt{2}\, v', \qquad w_{max} = \sqrt{2}\, w'$$

for turbulent fluctuations. For want of a better procedure, A and B were determined by this method, and were found to

increase with increasing ΔU_{max} and $\Delta\varphi_{max}$. Denoting the values of A given by equations (11) and (13) by A_{11} and A_{13} and the value of B given by equation (12) by B_{12}, the errors as given in table I are found.

TABLE I

$\frac{u'}{U}$, $\frac{v'}{U}$, $\frac{w'}{U}$	Wire normal to wind	Wire 45° to wind	
	$\frac{A-A_{13}}{A_{13}}$ (percent)	$\frac{A-A_{11}}{A_{11}}$ (percent)	$\frac{B-B_{12}}{B_{12}}$ (percent)
0.05	Too small to estimate	Too small to estimate	Too small to estimate
.10	0.2	Too small to estimate	1.0
.15	1.5	1.0	5.0
.20	7.0	5.0	9.0
.25	12.5	9.0	14.0
.30	19.0	15.0	20.0
.35	27.0	20	-

The errors were found to depend on the velocity to a slight extent, but not enough to warrant consideration in a table of this sort, which, after all, is intended mainly to indicate the order of magnitude of the errors.

The errors indicated in column 2 apply to a measurement of u'/U. They are in such a direction as to make the measured value too high by the percentages given. The errors indicated in columns 3 and 4 apply to the measurement of shearing stress. According to equation (20) the error in the shearing stress is the error in A_{11} plus the error in B_{12} for the appropriate values of u'/U and v'/U. Again the error

is in such a direction as to make the measured shearing stress too high.

Before investigating the error in correlation coefficient, it is noted that errors in v'/U and w'/U are not those indicated in column 4 of table I. The controlling factor here is the shape of the broken curve in figure 14. If the amplitude of the fluctuation does not go beyond the liner portion of this curve, the only error in v'/U and w'/U associated with size arises from the assumption that v/U and w/U are given by $\Delta\varphi$ when actually they are given by $\tan\Delta\varphi$. This error will generally be negligible for amplitudes that lie within the linear portion of the curve. According to figure 14, the amplitude of a sinusoidal fluctuation will go beyond the linear portion when v'/U or w'/U exceeds 0.19. It will be assumed that the error arising from u'/U may be corrected by means of equation (37), and v'/U and w'/U will be regarded as being free from error due to size for values up to 0.19. It will be necessary to pass over the question of errors for values greater than 0.19.

If no error in v' is assumed, it will be possible to get some idea of the error in correlation coefficient from table I. It is found, for example, that the error in K_1 (equation (24)) is given approximately by the difference between the errors in A_{13} and A_{11} in columns 2 and 3. The error in K_2 (equation(25)) reaches about 2 percent for a value of 0.3 in column 1. The error in K_3 (equation (27)) is the error in shearing stress minus that in u'.

At the 22-foot position the maximum value of u'/U is found from figure 22 to be 0.19. If u' and v' are in the same ratio here as at the 17½-foot position, the predicted v'/U will be about 0.11. The errors charged to size in measurements at the point nearest the surface in the 22-foot position are estimated to be:

6 percent in	u'/U
6 percent predicted in	c_f
Not more than 1 percent predicted in	K
No error predicted in	v'/U and w'/U

According to reference 9 there is an error in compensation involved in the use of expression (39), which depends on

the size of a term

$$2\pi f a M$$

where a is the amplitude of the resistance changes divided by $R-R_a$. It is shown that the error is less than 2 percent when $2\pi f a M$ is no greater than 0.14. Since the distribution of amplitude with frequency in a turbulent boundary layer is not known, no estimate of the actual error can be made. The fact that an error in compensation is likely to enter to a greater and greater degree as the fluctuations increase in size is further argument for using wires of the smallest possible diameter.

X. CONCLUSIONS

An account has been given of the recent developments in hot-wire instruments for use in turbulent boundary layers. From the theory of hot-wire measurements and the characteristics of the various instruments it is concluded that u', v', w', $\overline{uv}$, and K may be measured. These quantities are among the more important characteristics of the turbulence needed to further an understanding of turbulent boundary layers. The results so far obtained in the boundary-layer investigation for which the instruments were developed show that these quantities can be measured in the thick turbulent boundary layer used in the present experiment. The average characteristics of the layer are shown by the pressure distribution, mean velocity distribution, thickness, and separation point.

More observations are necessary before the experimental uncertainties can be properly appraised. In theory at least, the important errors are those that increase with the relative magnitude of the fluctuations and are inherent in the constant-current method of operating hot-wire anemometers. The relations between the voltage and the magnitude and direction of the wind are not linear; and it is for this reason that the proportionality factors A and B are not constant, but are rather some involved function of the root-mean-square value of the fluctuations. This fact has long been recognized, but has never been a serious drawback in the measurement of free-stream turbulence where the fluctuations rarely exceed a few percent of the mean velocity. These errors are a matter of concern in boundary-layer applications, but are not sufficient to condemn the method. They do, however, show the need for

further development of other methods of operation that are better adapted to the measurement of large fluctuations, such as the constant-temperature method with linearizing circuits proposed by Weske in reference 11.

National Bureau of Standards
Washington, D. C., June 29, 1945.

REFERENCES

1. von Kármán, Th.: Turbulence and Skin Friction. Jour. Aero. Sci., vol 1, no. 1, Jan. 1934, pp. 1-20.

2. Schubauer, G. B.: A Turbulence Indicator Utilizing the Diffusion of Heat. NACA Rep. No. 524, 1935.

3. Taylor, G. I.: Diffusion by Continuous Movements. Proc. London Math. Soc., vol 20, Aug. 1921, pp. 196-211.

4. Dryden, Hugh L.: Turbulence Investigations at the National Bureau of Standards. Proc. Fifth Int. Cong. Appl. Mech., Cambridge, Mass., 1938, pp. 362-368.

5. Dryden, Hugh L., Schubauer, G. B., Mock, W. C., Jr., and Skramstad, H. K.: Measurements of Intensity and Scale of Wind-Tunnel Turbulence and Their Relation to the Critical Reynolds Number of Spheres. NACA Rep. No. 581, 1937.

6. Weske, John R.: Methods of Measurement of High Air Velocities by the Hot-Wire Method. NACA TN No. 880, 1943.

7. Mock, W. C., Jr.: Alternating-Current Equipment for the Measurement of Fluctuations of Air Speed in Turbulent Flow. NACA Rep. No. 598, 1937.

8. Mock, W. C., Jr., and Dryden, H. L.: Improved Apparatus for the Measurement of Fluctuations of Air Speed in Turbulent Flow. NACA Rep. No. 448, 1932.

9. Dryden, H. L., and Kuethe, A. M.: The Measurement of Fluctuations of Air Speed by the Hot-Wire Anemometer. NACA Rep. No. 320, 1929.

10. Dryden, Hugh L.: Isotropic Turbulence in Theory and Experiment. Appl. Mechanics, Theodore von Kármán Anniversary Vol., May 11, 1941, pp. 85–102.

11. Weske, John R.: A Hot-Wire Circuit with Very Small Time Lag. NACA TN No. 881, 1943.

12. King, L. V.: On the Convection of Heat from Small Cylinders in a Stream of Fluid: Determination of the Convection Constants of Small Platinum Wires with Applications to Hot-Wire Anemometry. Phil. Trans. Roy. Soc., London, ser. A, vol. 214, 1914, pp. 373–432.

13. von Doenhoff, Albert E., and Tetervin, Neal: Determination of General Relations for the Behavior of Turbulent Boundary Layers. NACA ACR No. 3G13, 1943.

Figure 1.- Front view of "boundary-layer wall" in 10-foot wind tunnel. Height of wall is 10 feet. Instrument support shown on working side.

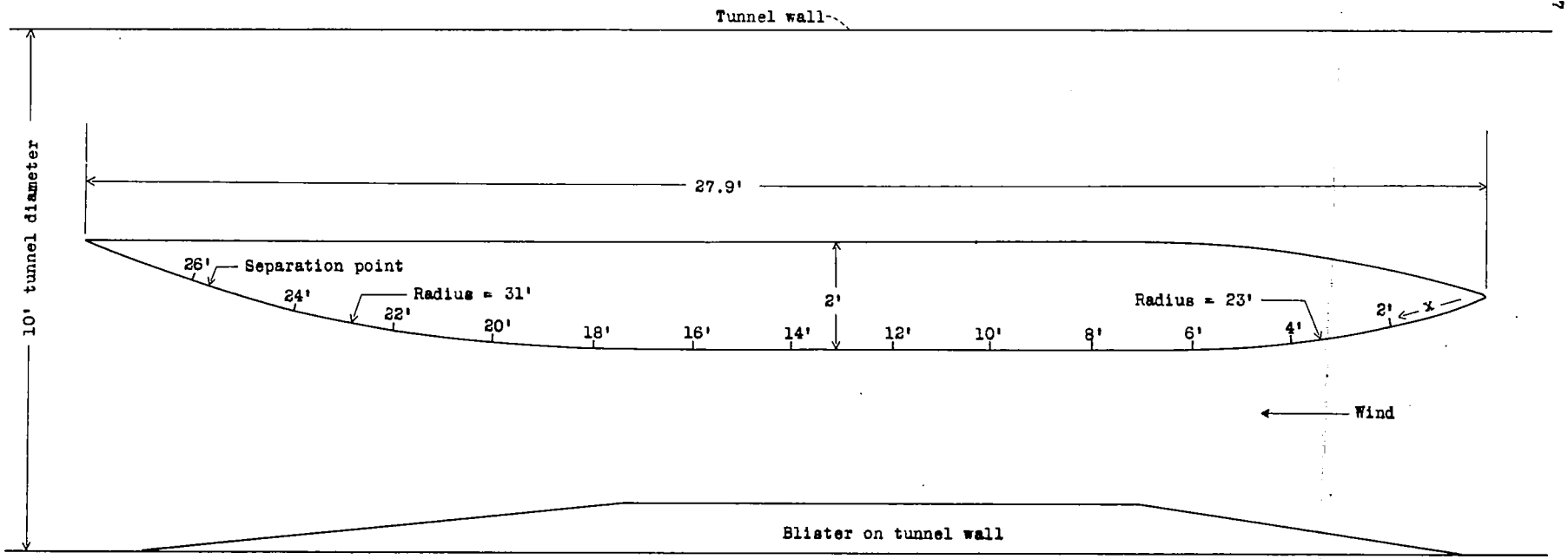

Figure 2.- Diagram of "boundary-layer wall" with scale of x on working side.

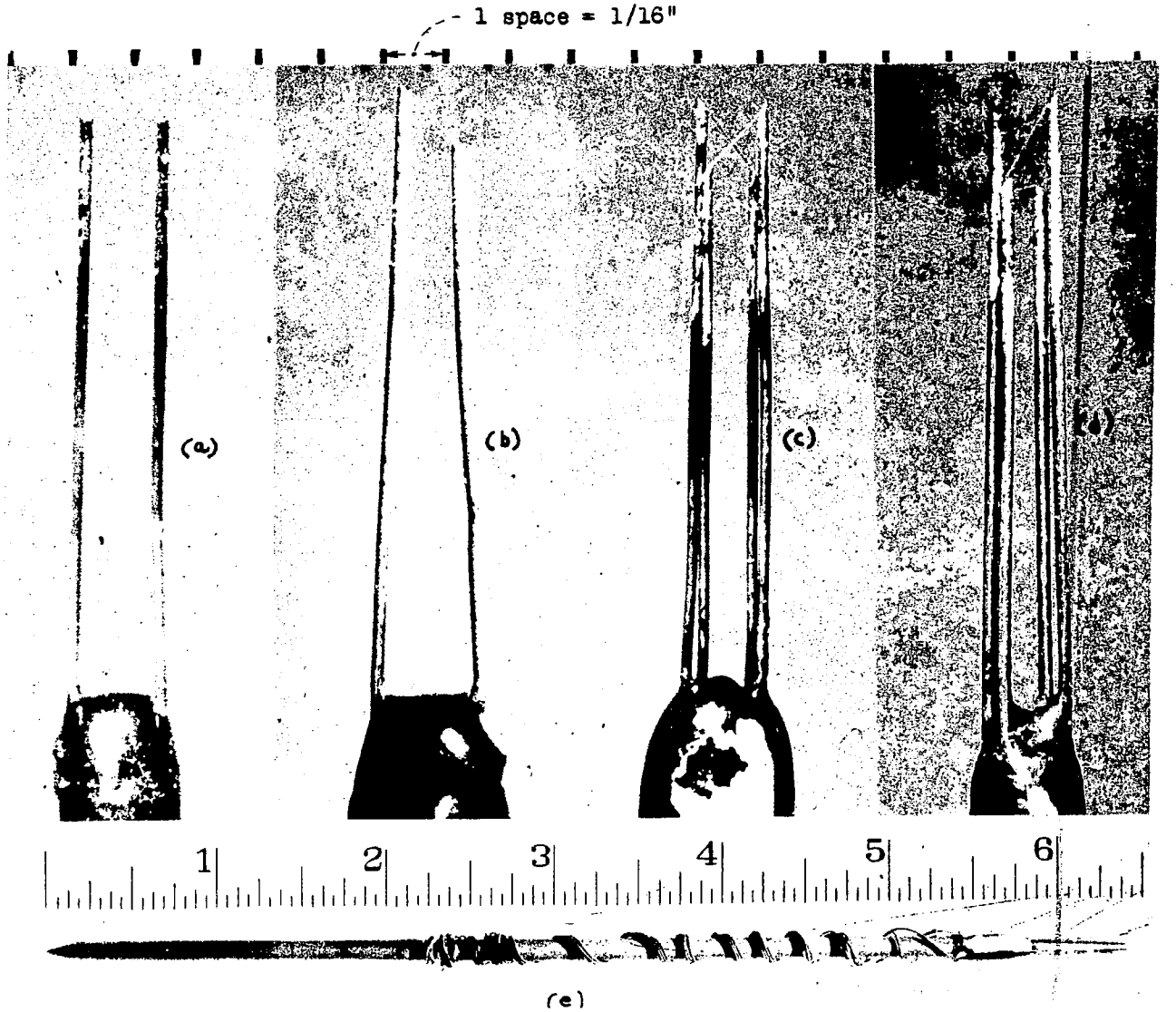

Figure 3.- Magnified view of hot-wire arrangements. (a), arrangement for measuring u'; (b),(c), arrangements for measuring turbulent shearing stress; (d), arrangement for measuring v' and w'; (e), one complete instrument. Actual size of (a),(b),(c),(d) shown by larger 1/16-inch scale divisions, actual size of (e) shown by smaller 1/16-inch scale divisions.

METHOD FOR ELECTROPLATING TUNGSTEN WIRE

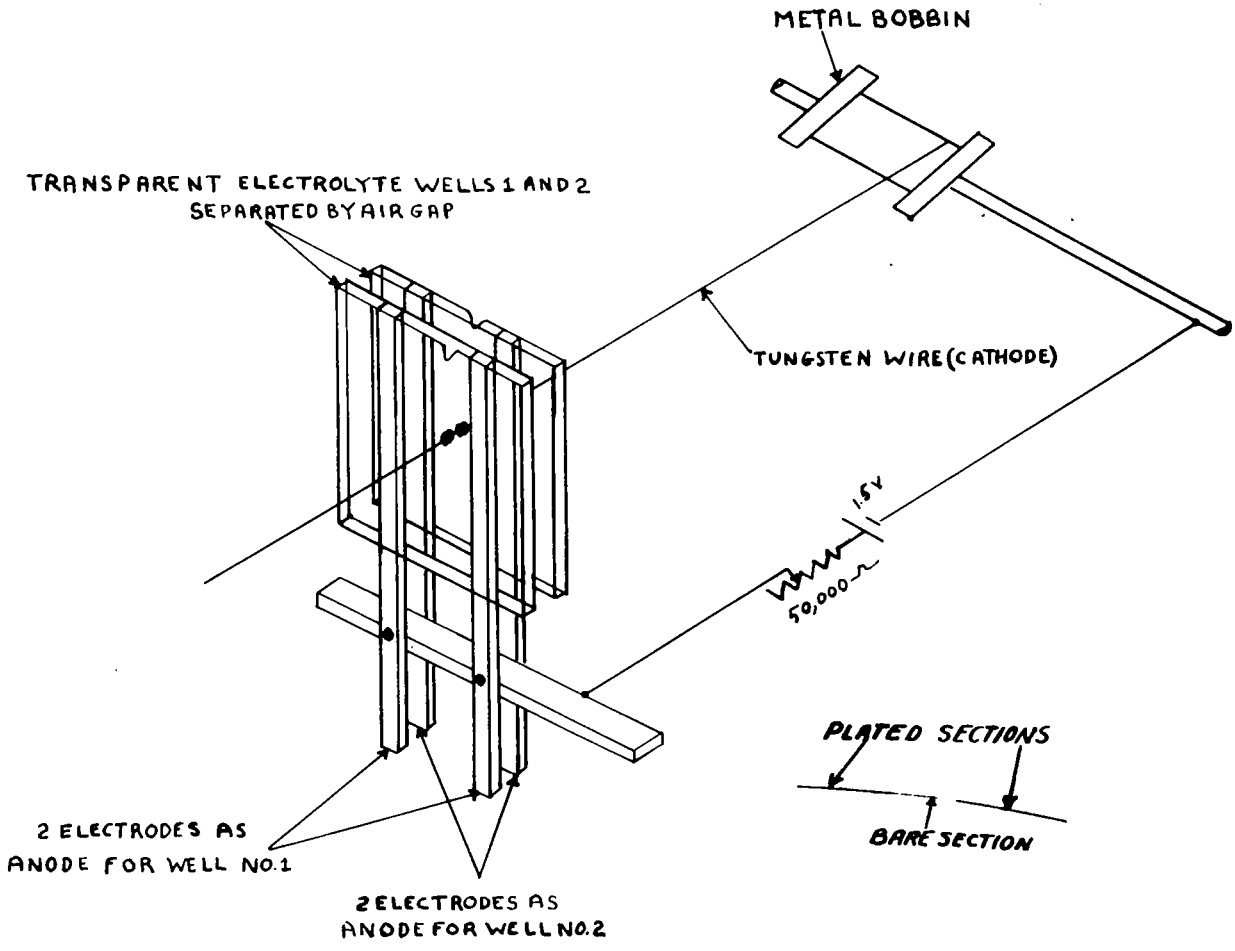

Figure 4.- Electroplating bath. Insert shows a microphotograph of 0.00031-inch diameter tungsten wire with plated sections.

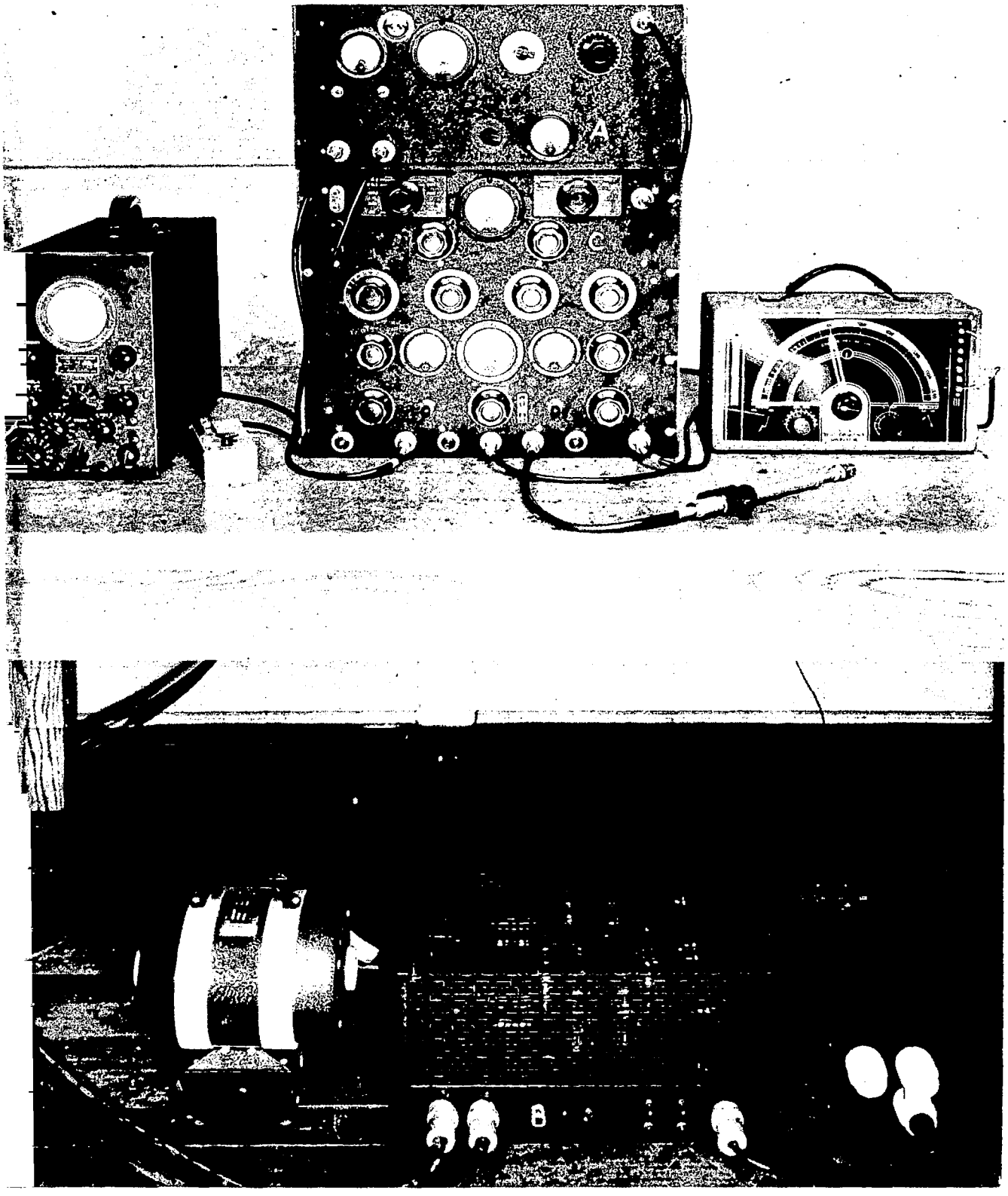

Figure 5.- Assembled electrical equipment. A, amplifier; B, power supply; C, control unit.

PORTABLE TURBULENCE MEASUREMENT EQUIPMENT

CONTROL UNIT

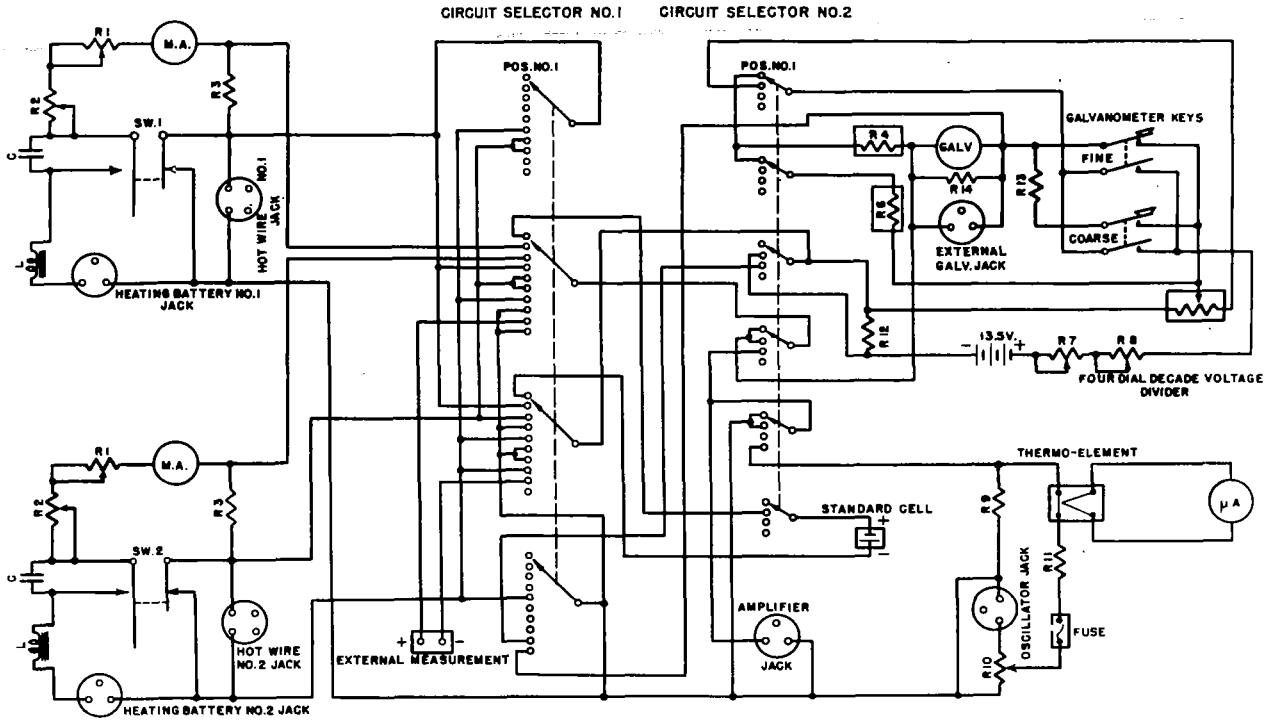

CONTROL UNIT COMPONENTS

R1,	6	ohms
R2,	200	"
R3,	10	"
R4,	100	"
R5,	1,000	" 4 dial decade
R6,	1,000	"
R7,	100	"
R8,	500	"
R9,	Special resistor adjusted to give 0.0025 volt drop when carrying 1/2 scale oscillator meter current.	
R10,	1,000	ohms
R11,	250	"
R12,	5,000	"
R13,	10,000	"
R14,	1,000	"
C,	0.5	mf.
L,	12	henries, 105 ohms.

Figure 6.- Diagram of control-unit circuit.

PORTABLE TURBULENCE MEASUREMENT EQUIPMENT
AMPLIFIER

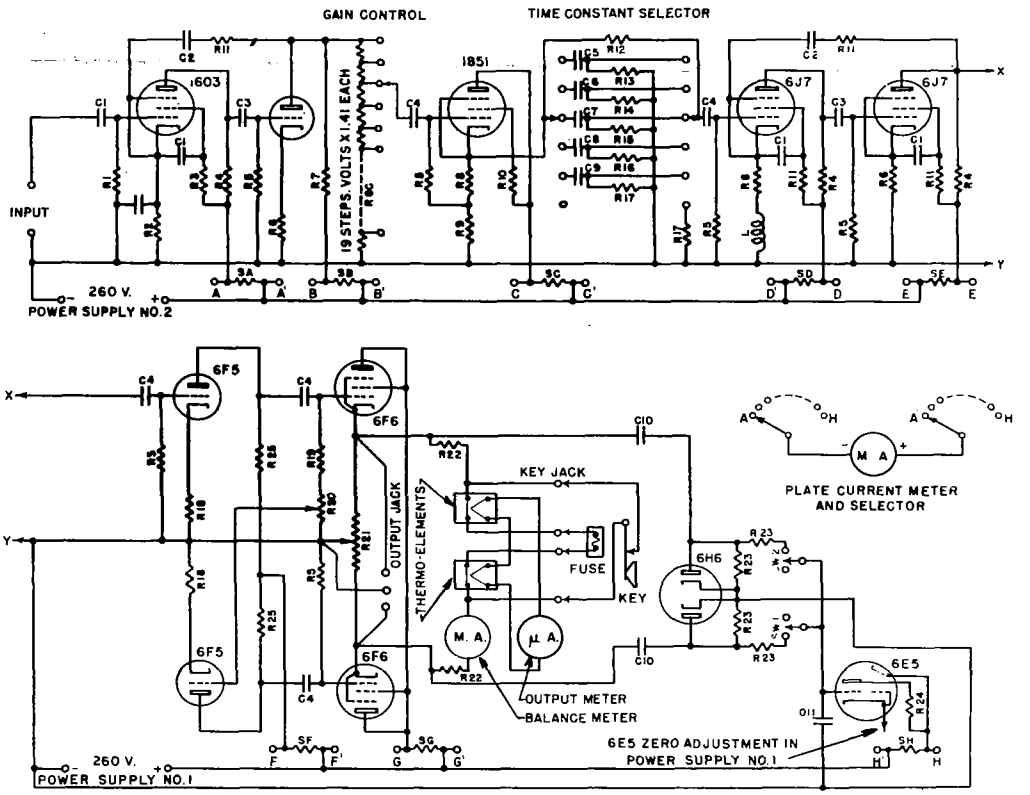

AMPLIFIER COMPONENTS

R1	100,000 ohms	R14	2,500 ohms
R2	2,000 "	R15	3,333 "
R3	2,000,000 "	R16	5,000 "
R4	500,000 "	R17	10,000 "
R5	3,000,000 "	R18	3,500 "
R6	1,000 "	R19	2,000,000 "
R7	25,000 "	R20	1,000,000 "
R8	150 "	R21	1,500 "
R9	750 "	R22	500 "
R10	50,000 "	R23	10,000,000 "
R11	1,000,000 "	R24	1,000,000 "
R12	1,000,000 "	R25	500,000 "
R13	2,000 "	RGC	10,240 ohms total

SA,	2 ma. full scale meter shunt
SB,	20 " " " " "
SC,	20 " " " " "
SD,	2 " " " " "
SE,	2 " " " " "
SF,	2 " " " " "
SG,	200 " " " " "
SH,	10 " " " " "

C1,	2 mf.	C5,	0.005 mf.	C9,	0.001 mf.
C2,	4 "	C6,	0.004 mf.	C10,	0.1 "
C3,	0.02 "	C7,	0.003 "	C11,	0.01 "
C4,	0.04 "	C8,	0.002 "	C12,	0.02 "

C13, 16 mf.
L, 60 millihenry

Figure 7.- Diagram of amplifier circuit.

PORTABLE TURBULENCE MEASUREMENT EQUIPMENT

POWER SUPPLIES

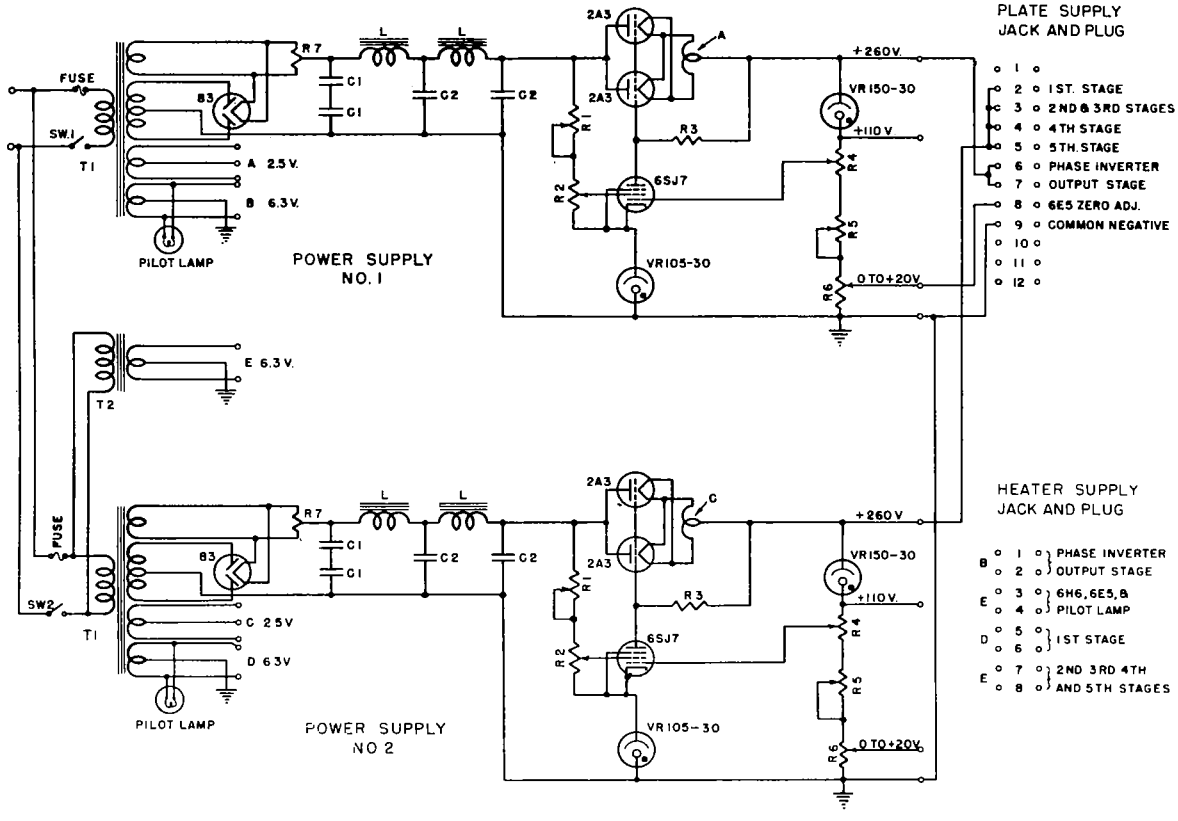

POWER SUPPLY COMPONENTS

R1,	15,000	ohms
R2,	10,000	"
R3,	250,000	"
R4,	1,000	"
R5,	10,000	"
R6,	3,500	"
R7,	20	" center tapped
C1,	8	mf.
C2,	32	"
C3,	0.5	"
L,	12 henries, 231 ohms	

T1, 750 Vac. center tapped, .18A; 5V., 3A.; 6.3V, 3.3A.; 2.5V., 6A.

T2, 6.3V., 3A.

Figure 8.- Diagram of power-supply circuit.

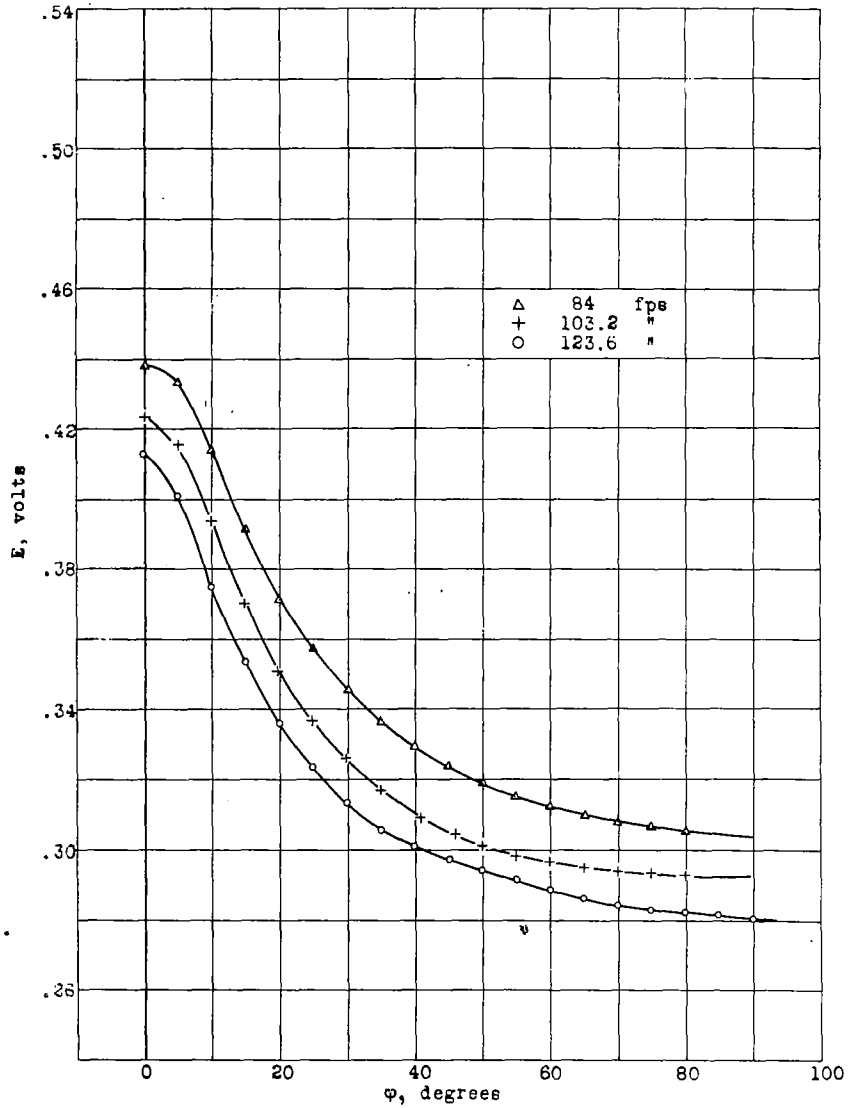

Figure 9.- Curves showing variation of voltage with angle at three wind velocities. E = voltage across wire, φ = angle between axis of wire and wind.

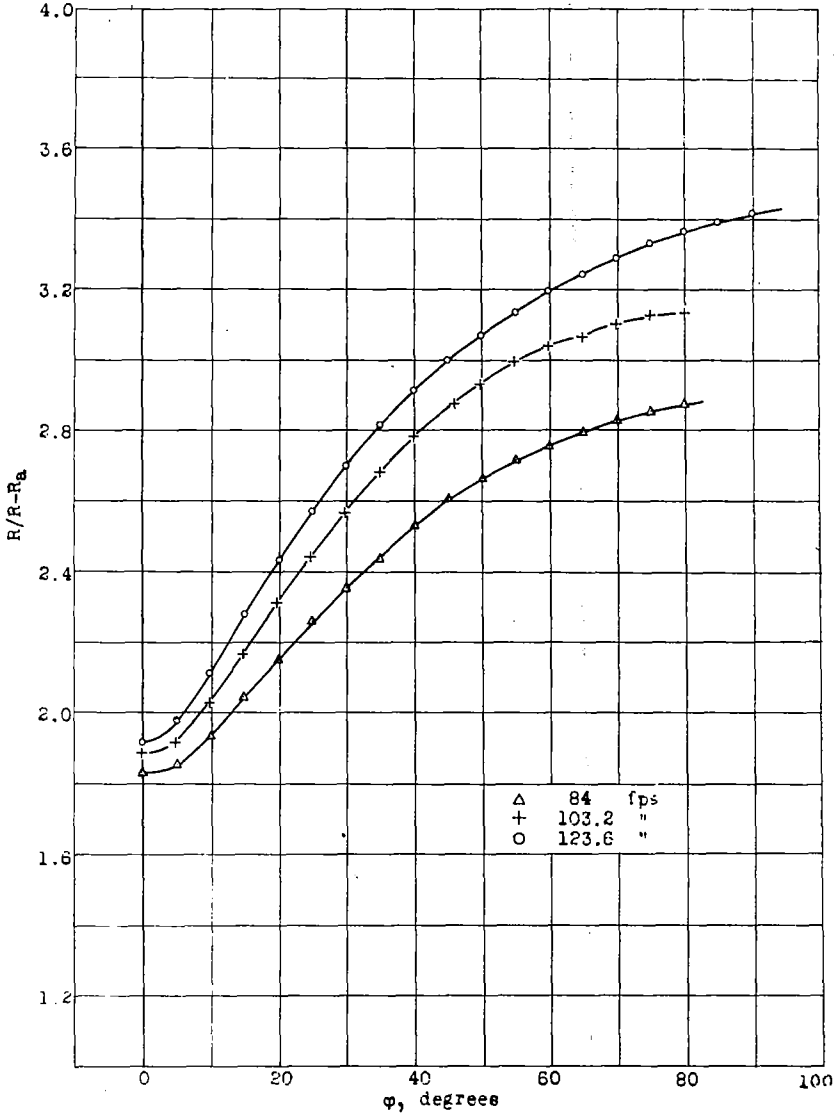

Figure 10.- Curves showing variation of $R/R-R_a$ with angle at three wind velocities. R = resistance of wire when heated, R_a = resistance of wire at air temperature, φ = angle between axis of wire and wind.

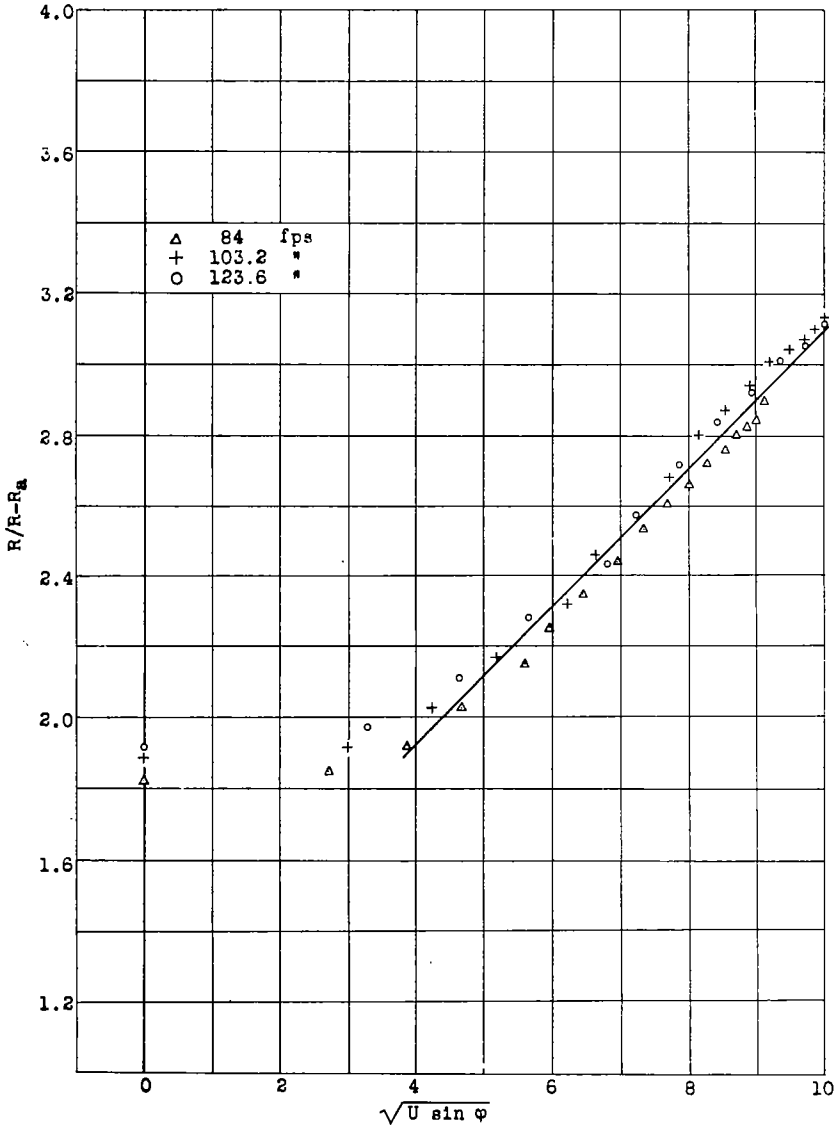

Figure 11.- Diagram showing linear relation between $R/R-R_a$ and $\sqrt{U \sin \varphi}$ (equation 7).

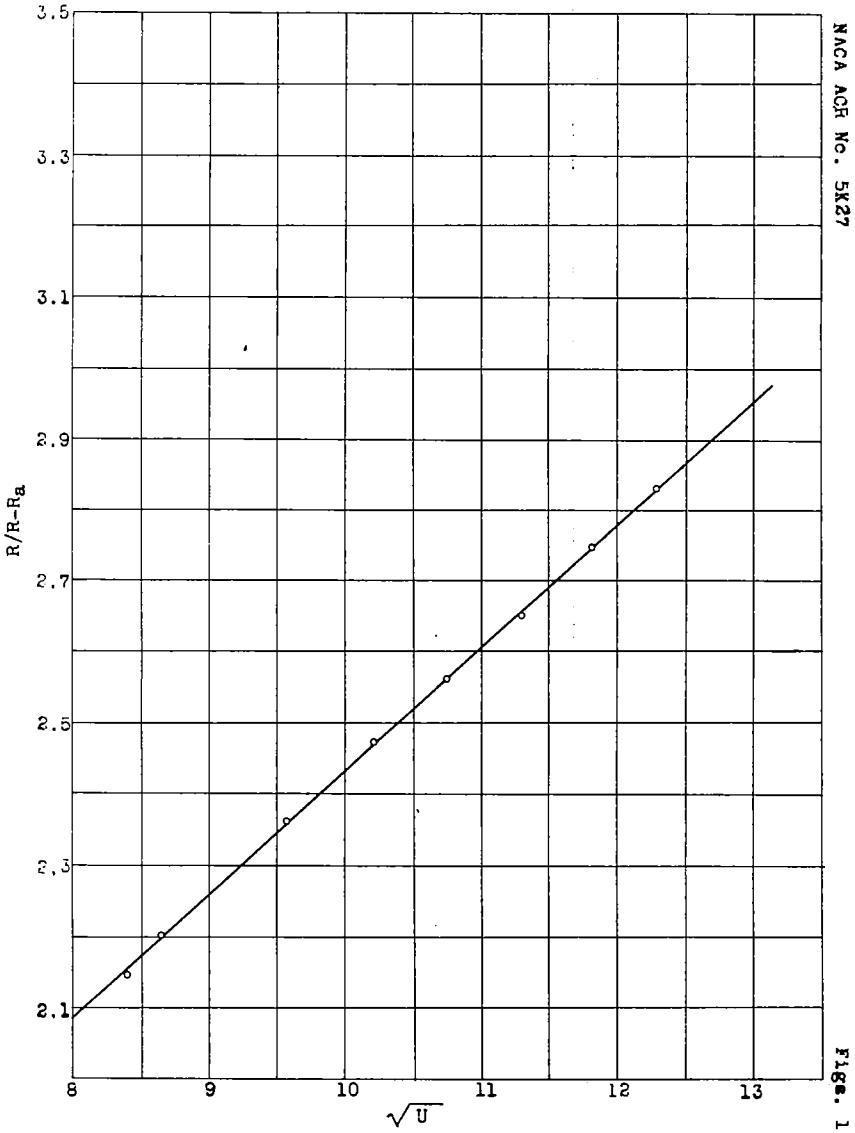

Figure 12.- Diagram showing linear relation between $R/R-R_a$ and $\sqrt{U}$ when $\varphi = 90$ degrees (equation 6).

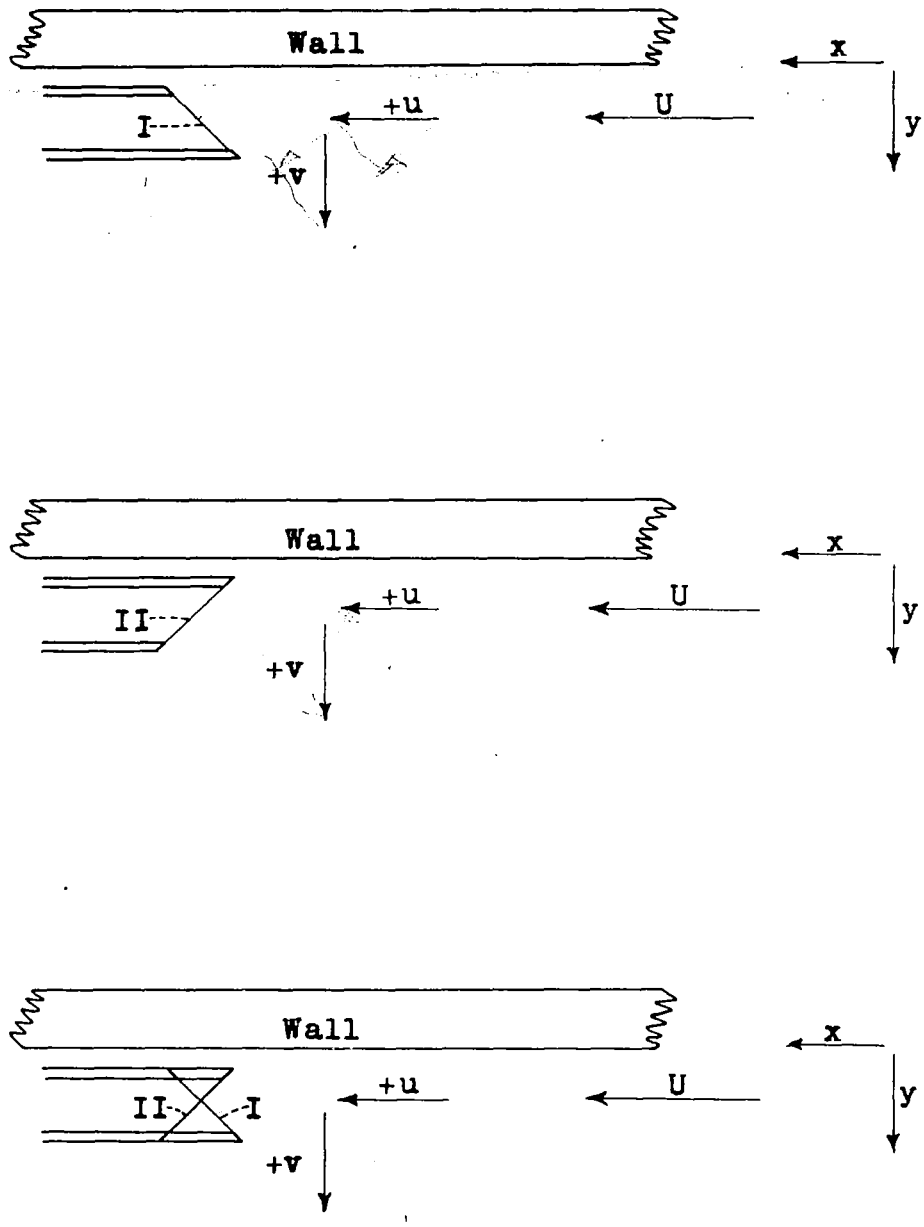

Figure 13.- Diagram illustrating position of wires for a measurement of turbulent shearing stress. Arrows indicate positive direction of x, y, U, u, and v.

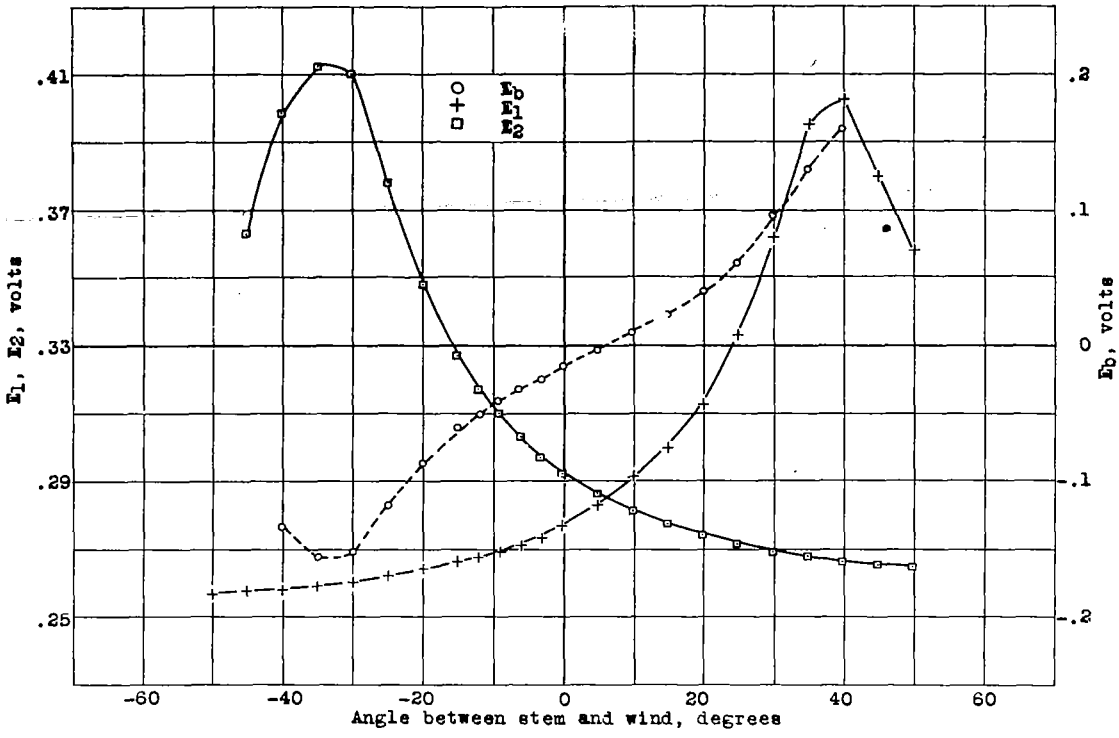

Figure 14.- Voltages E_1 and E_2 across each wire of an x-wire arrangement and difference voltage E_b at various angles. U = 124 feet per second.

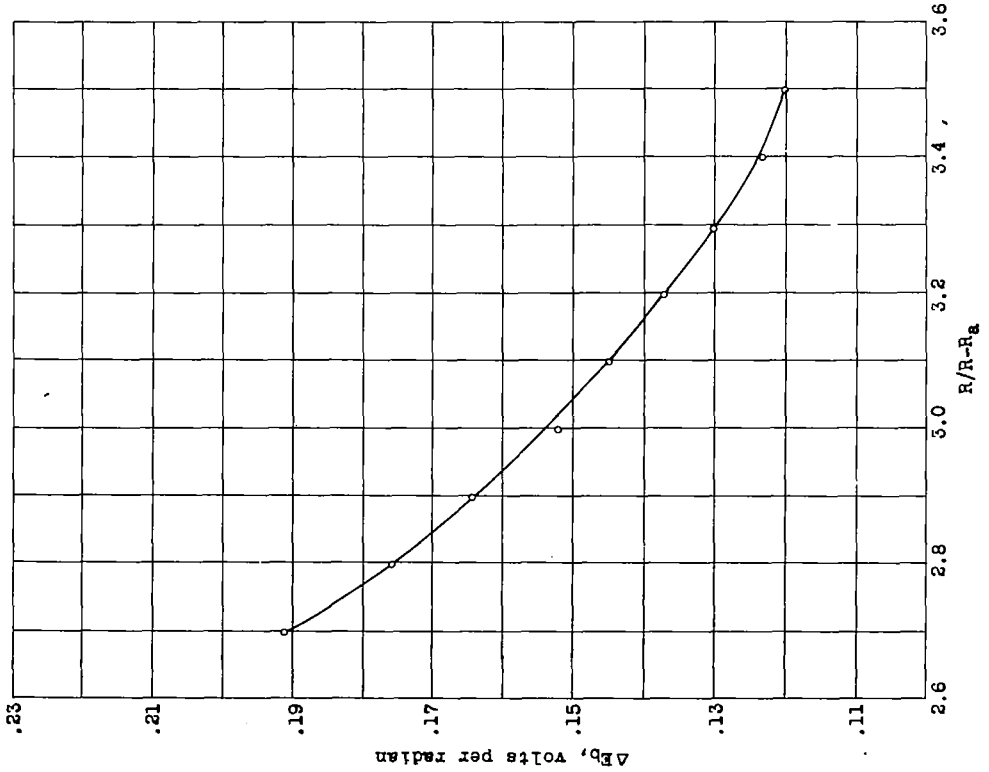

Figure 15.- Calibration curve used in the determination of v' and w'.

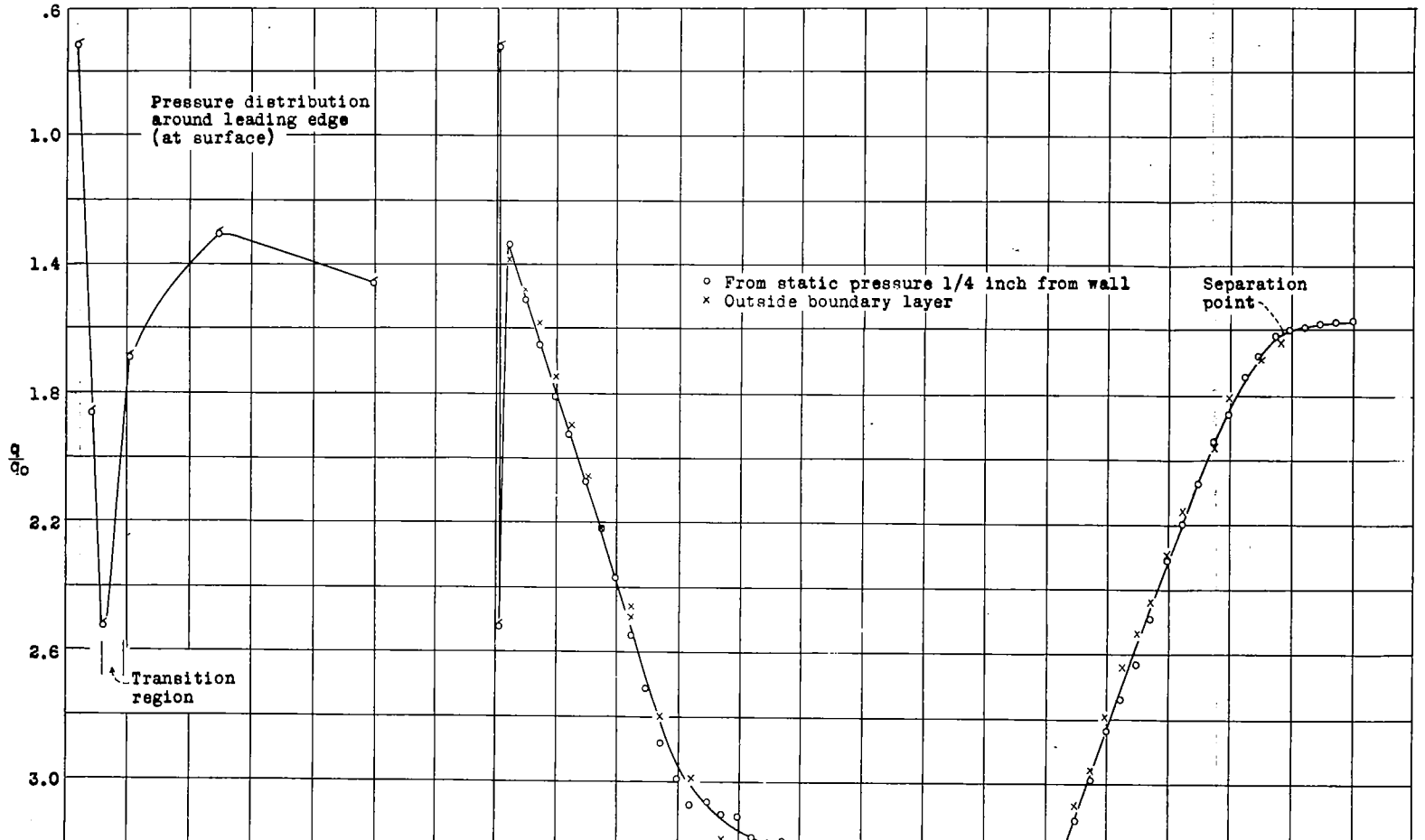

Figure 16.- Distribution of dynamic pressure at outer limit of boundary layer derived from static pressure measurements.

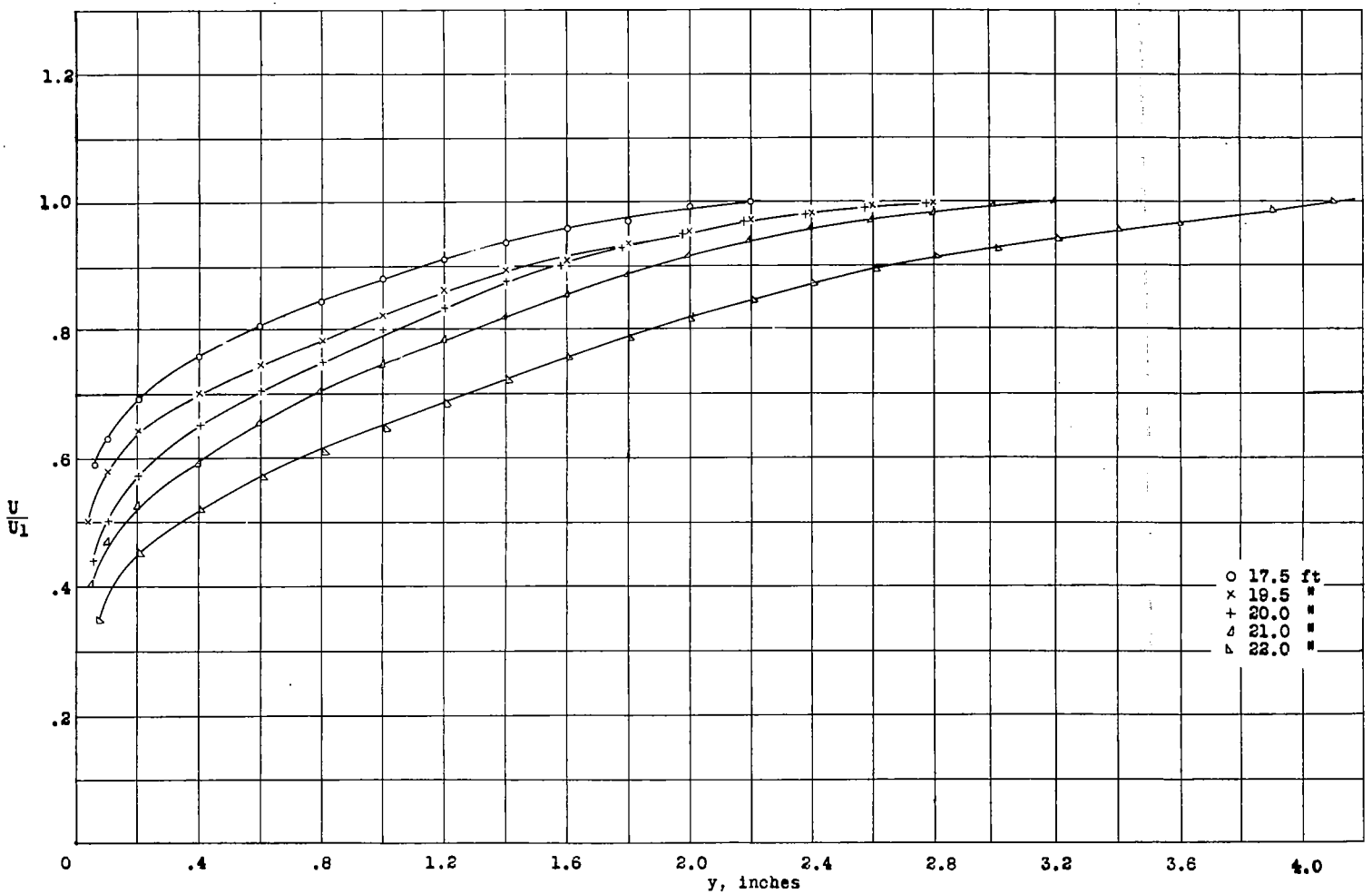

Figure 17.- Distribution of mean velocity determined by the hot-wire method.

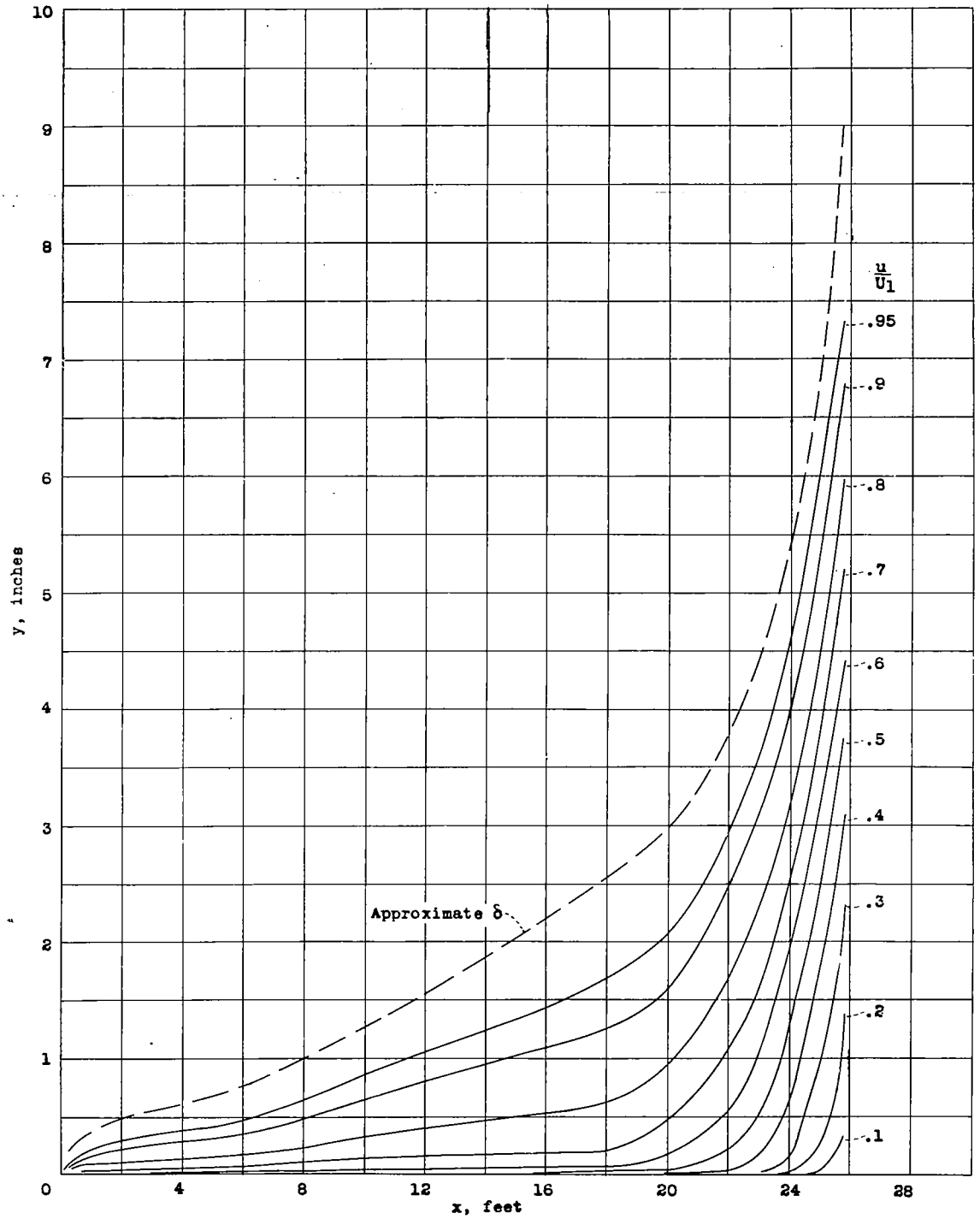

Figure 18.- Mean-velocity contour lines and outer limit of boundary layer. δ = boundary layer thickness.

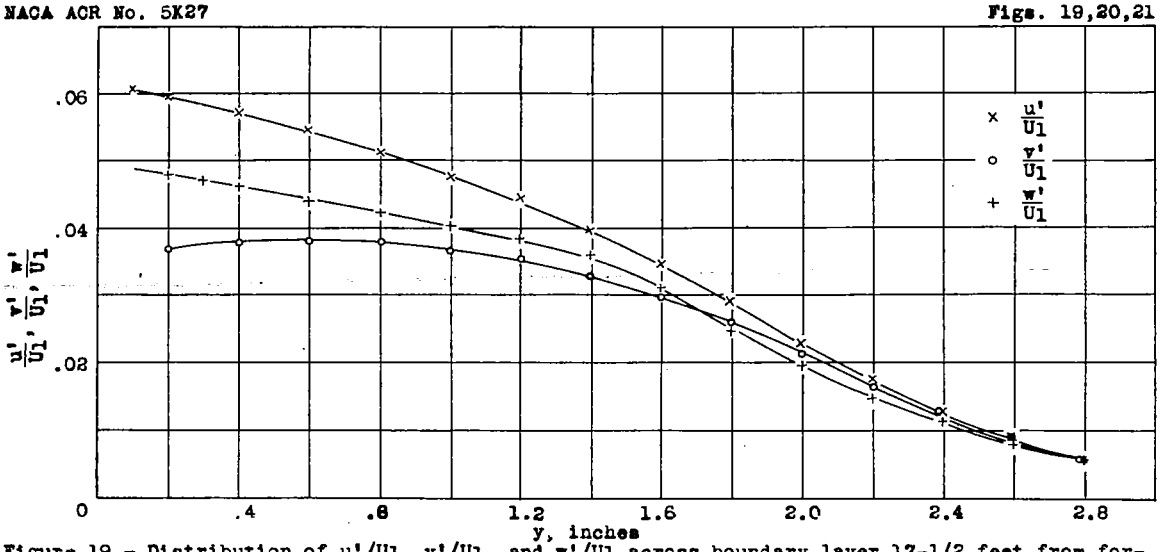

Figure 19.- Distribution of u'/U1, v'/U1, and w'/U1 across boundary layer 17-1/2 feet from forward stagnation point.

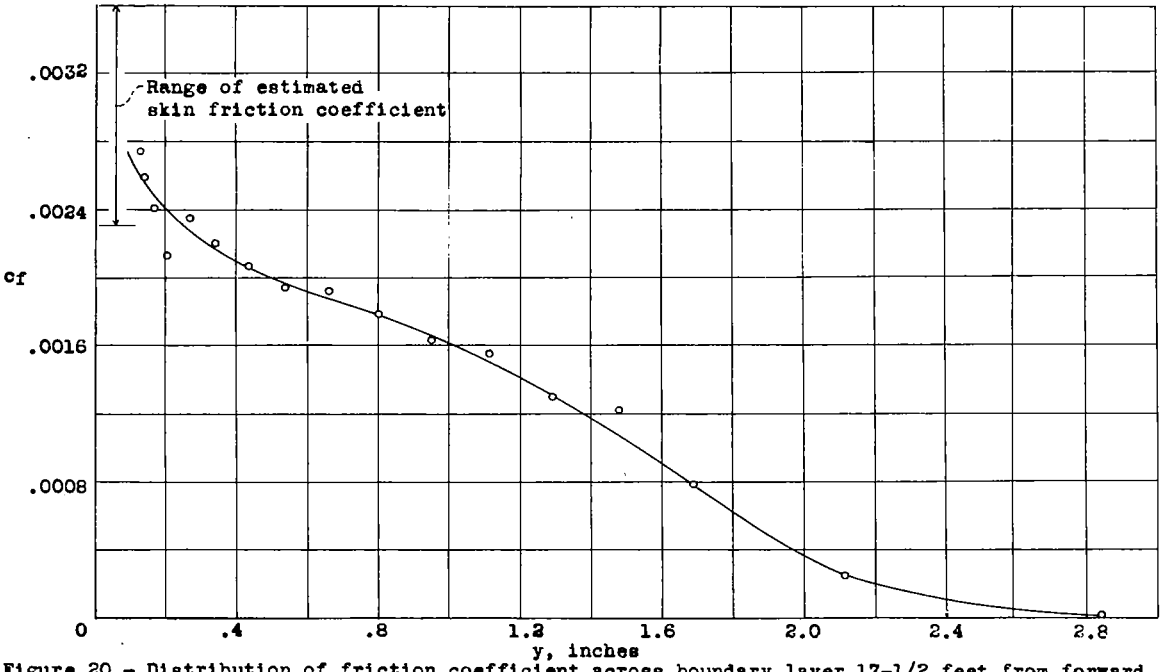

Figure 20.- Distribution of friction coefficient across boundary layer 17-1/2 feet from forward stagnation point. $c_f = 2\ \overline{uv}/U_1^2$.

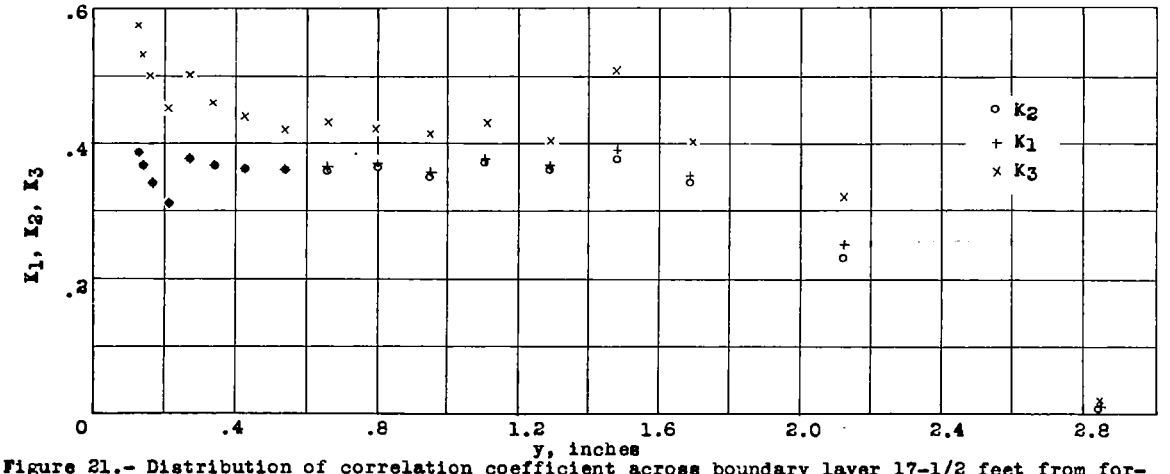

Figure 21.- Distribution of correlation coefficient across boundary layer 17-1/2 feet from forward stagnation point. $K = \overline{uv}/u'v'$. K_1, K_2, and K_3, values obtained from equations (24), (25), and (27) respectively.

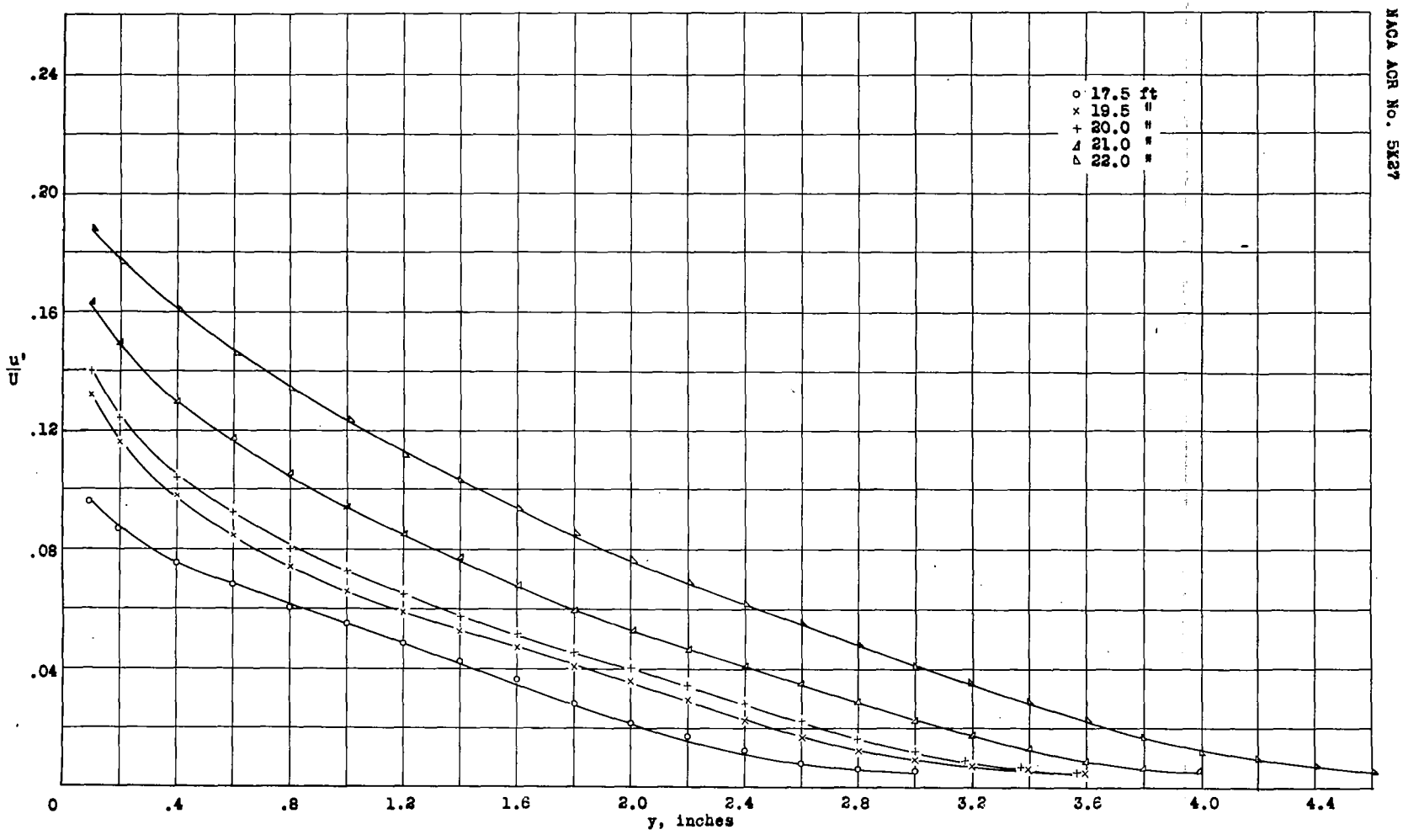

Figure 22.- Distribution of u'/U across the boundary layer at several distances x from the forward stagnation point.